

A Technical Report

Investigation on occurrences of extreme rain events across Northwest Himalaya in relation to global atmospheric thermal and circulation changes

Project Team

Dr. Ashwini Ranade (PI)

Dr. P.K. Mishra & Dr. Sunil Gurrapu (Co-PI)

Center for Cryosphere and Climate Change Studies
National Institute of Hydrology, Roorkee- 247667



Year 2022-25

CONTENTS

Abstract	3
List of Figures	4
List of Tables.....	5
List of Abbreviations	6
1. Introduction	7
2. Study Area and dataset used	9
3. Methodology	10
4. Analysis and results	
4.1. Annual and seasonal rainfall characteristics across NW Himalaya	11
4.1.1 Long-term trend and recent year changes	12
4.2 Identification of large-scale extremes concerning rainfall amount (ERE-RA) and rainwater (ERE-RW)	15
4.3 Long-term trends and recent changes in parameters of large-scale Extremes	18
4.4. Identification and characteristics of small-scale isolated spatio- temporal extremes (ST-EREs)	22
4.5 Trend analysis of rainfall and frequency of occurrences of ST-EREs	23
4.6 elevation dependant occurrences of ST-EREs	25
4.7 Weather systems associated with rain/snow over NW Himalaya	26
4.8 Composite meteorological analysis of most extreme LS-EREs in different seasons.	27
4.8.1 Most Extreme LS-EREs during winter	27
4.8.2 Most Extreme LS-EREs during Monsoon	35
4.8.3 Key differences between winter and monsoon LS-EREs	44
5. Important Results	45
6. Conclusions	46
7. Implications to regional hydrology and disaster risk management.....	46
References	48

ABSTRACT

Heavy rain events over the northwest Himalayan region are becoming ferocious in recent years causing catastrophic disasters. Climatological and fluctuation features of annual and seasonal rainfall of NWH comprising Uttarakhand (UK), Himachal Pradesh (HP) and Jammu and Kashmir (J&K) states are studied in details during 1951-2021 using IMD's 0.25° gridded rainfall data. The large-scale extreme rain events (LS-EREs) are also calculated over NWH and the three states. The analysis reveals distinct rainfall trends across the NWH states over the period, with notable variations in recent decades. In UK, no significant long-term trend is seen in annual or monsoonal rainfall, but October–November (OND) rainfall has declined by 35% over the past 20 years. HP shows a significant 13% reduction in annual rainfall, with OND, JF, and MAM rainfall declining by 33%, 17%, and 17%, respectively. In contrast, J&K exhibits a long-term increase in JF rainfall and an 18% rise in monsoonal rainfall in the last 20 years.

The LS-EREs intended to quantify the severity of persisting intense rains causing severe flood and damage. For NWH as a whole, while no significant change is observed in the rainfall amount (RA) of EREs, notable changes have occurred in other metrics over the past 20 years. Their areal extent (AE) increased by 28–43%, and 1-day rainwater (RW) contribution rose by 16%. At state-level, UK saw a 10–23% increase in RA and up to 34% in RW; J&K experienced 16–23% increases; HP observed a 10–20% decrease in RA and up to 19% decline in RW. Short-duration EREs (1–3 days) have become more frequent and intense in high-altitude areas of J&K and northern UK, while decreasing trends are seen in mid-/low-altitude HP and southern UK. Most severe events occur below 3000 m elevation. Low-intensity EREs are widespread, with higher frequencies in J&K, while high-intensity EREs are less common and concentrated in northern J&K and high-altitude southern areas of HP and UK. Most of the severe ST-EREs of the length up to 3-days are observed to occur below 3000m of elevation mostly in the states of HP and UK.

Wintertime most severe LS-EREs are largely associated with deep western disturbances, significantly modulated by interaction with the south-westerly jet stream. However, convective mechanisms associated with persistence in temperature and circulation anomalies are observed to be strongly linked to the occurrences of LS-EREs during monsoon season. This study provides insight into the changing patterns of large-scale extreme rainfall events in the Himalayas, which significantly impact river flows, groundwater recharge, and reservoir management. The results will be helpful for predicting flood risks, planning for sustainable water resource allocation, and improving the resilience of hydrological systems to climate-induced changes.

Keywords: large-scale extreme rain events, Himalayan extremes, winter extremes, monsoon extremes, meteorological conditions for Himalayan extremes.

LIST OF FIGURES

Figure 1. Study area: Northwest Himalaya

Figure 2. Methodology adopted for the analysis of Extreme rain events across NWH

Figure 3. Spatial distribution of climatological mean (top) and maximum (bottom) of annual and seasonal rainfall across NWH

Figure 4. Interannual variations and recent 20 year changes in annual and seasonal rainfall across NWH and three states

Figure 5. Spatial variations in Long-term trend in annual and seasonal rainfall during 1951-2021

Figure 6 Spatial distribution of daily mean monsoon rainfall across NWH

Figure 7. Seasonal distribution of year-wise most severe 1-day large-scale ERE-RA and ERE-RW occurrences

Figure.8 Interannual variations in rainfall amount of large-scale ERE-RA over NWH and three states

Figure.9 Interannual variations in rainwater of large-scale ERE-RW over NWH and three states

Figure 10. Relationship of Rainfall Amount (a) and Rainwater (b) with the duration of 1- to 25-day EREs over NWH

Figure 11. Spatial variation in mean rainfall amount of 1-to 10-day ST-EREs and that for most Extreme ST-EREs

Figure 12. Annual and monsoonal mean frequency of occurrences of 1-day Extremes of different intensities

Figure 13. spatial distribution of long-term trend in rainfall of 1-to 10-day ST-EREs during 1951-2021

Figure 14. (a) Spatial distribution of long-term trends in annual frequency of 1-day ST-EREs of different intensities; and (b) that for monsoon season

Figure 15. Mean rainfall intensity of 1- to 3-day ST-EREs and elevation (above 3000m).

Figure 16. Rainfall field during most severe LS-EREs during winter season of 1951-2023

Figure 17. Composites of temperature Anomalies at 850 hpa, and 200hpa prior to, during and after the occurrences of LS-ERE over NWH during Winter

Figure 18 . Composites of geopotential height Anomalies at 850 hpa, 500hPa and 200hpa prior to, during and after the occurrences of LS-ERE over NWH during Winter

Figure 19. Composites of tropospheric temperature and thickness anomalies prior to, during and after the occurrences of LS-ERE over NWH during Winter

Figure 20. Composites of wind anomalies and relative vorticity at 500hPa and 200hPa prior to, during and after the occurrences of LS-ERE over NWH during winter

Figure 21 Normal Global weather regimes at 850 hPa, 600hPa, 400hPa and 200hpa during winter and composites for the occurrences of LS-EREs over NWH during winter

Figure 22. Rainfall field during most severe LS-EREs during monsoon season of 1951-2023

Figure 23. Composites of temperature Anomalies at 850 hpa, and 200hpa prior to, during and after the occurrences of LS-ERE over NWH during monsoon

Figure 24 . Composites of geopotential height Anomalies at 850 hpa, 500hPa and 200hpa prior to, during and after the occurrences of LS-ERE over NWH during monsoon

Figure 25. Composites of tropospheric temperature and thickness anomalies prior to, during and after the occurrences of LS-ERE over NWH during monsoon

Figure 26. Composites of wind anomalies and relative vorticity at 500hPa and 200hPa prior to, during and after the occurrences of LS-ERE over NWH during monsoon

Figure 27 Normal Global weather regimes at 850 hPa, 600hPa, 400hPa and 200hpa during monsoon and composites for the occurrences of LS-EREs over NWH during monsoon

LIST OF TABLES

Table 1 Climatological characteristics of parameters of 1 to 10-day large-scale ERE-RA and ERE-RW over NWH

Table 2. Climatological characteristics (mean and SD) parameters of 1 to 10-day large-scale ERE-RA and ERE-RW over three states of NWH

Table 3. percentage change in recent 20 years (2001-2021) compare to preceding (1951-2000) period in parameters of large-scale EREs of 1- to 10-day durations

LIST OF ABBREVIATIONS

AE	Areal extent
CL	Cool-Low
CH	Cool-High
EREs	Extreme rain events
ERE-RA	Extreme rain event concerning rainfall amount
ERE-RW	Extreme rain event concerning rainwater
EC-T _{level}	Equatorially conditioned temperature at a particular level
EC-Z _{level}	Equatorially conditioned geopotential height at a particular level
EC-mslp	Equatorially conditioned mean sea level pressure
EC-ppw	Equatorially conditioned precipitable water
GC-W _{level}	Globally conditioned wind speed at a particular level
HP	Himachal Pradesh
JF	January-February
J&K	Jammu and Kashmir
JJAS	June-July-Aug-Sept
LS-EREs	Large-scale extreme rain events
mslp	Mean sea level Pressure
MK	Mann-Kendall
MAM	March-April-May
NWH	Northwest Himalya
OND	October-November-December
ppw	Precipitable water
RA	Rainfall Amount
RW	Rainwater
ST-EREs	Spatio-temporal extreme rain events
UK	Uttarakhand
WDs	Western Disturbances
WL	Warm-Low
WH	Warm-High

1. INTRODUCTION:

The Himalayan mountains serve as vital water reservoirs, sustaining millions downstream. However, in recent decades, the region has experienced unprecedented heavy rainfall, leading to devastating floods, landslides, and socio-economic losses. These events highlight the complex interplay between climate change and large-scale atmospheric systems. The northwest Himalayas, with their highly complex terrain and tropical-extratropical interactive atmosphere, are particularly prone to such extremes, especially during the monsoon season. They pose severe risks to the fragile ecosystem, traditional hydrological cycles and local communities. Research suggests that multiple factors driven by climate change contribute to extreme rainfall events. Interactions between deep westerly troughs, cross-equatorial Indian Ocean south-westerlies, and Pacific easterlies create large and intense monsoon troughs extending from the Philippines to the Indus Basin. These phenomena that involve confluence and convergence of huge air masses of contrasting characteristics are short-lived, resulting in rapid condensation and intense rainfall due to the confluence of contrasting air masses over the subtropical mountainous terrain. Colloquially termed as the cloudburst has a potential to downpour over a smaller region in very short duration. International disaster database (<http://www.emdat.be>) has reported the substantial increase in the extreme rain events over the western Himalayas in recent 30-40 years. It is one of the most studied but less understood phenomena so far. Under the influence of highly complex terrain and tropical-extratropical interactive atmosphere, the northwest part of Himalaya becomes more prone to such types of extreme events, especially during the monsoon season. Other parts of the country also experiencing extreme rain events each year surprisingly even during large-scale droughts also. In addition, there is a widespread belief that, in a recent global warming period, due to the intensification of the hydrological cycle, extreme rain events are increasing (Senior et al. 2002, IPCC 2007). The sixth assessment report (IPCC, 2021) projected that, extreme rainfall is projected to be intensifies by 7% for each additional 1 °C due to acceleration of hydrological cycle in warmer climate across the globe and become more frequent mostly in Africa and Asia. These changes heighten the risks of floods and droughts, intensifying the challenges of water resource management in a warming climate, particularly in regions like India where monsoons play a crucial role in agriculture, hydrology, and overall socio-economic stability.

Many studies have suggested the rising frequency of extreme rain events in Himalaya has mostly attributed to the following conditions: i) a significant increase in synoptic activities over the Bay of Bengal and Arabian sea; ii) anomalous convective instability; iii) atmospheric conditions over the equatorial Indian Ocean; iv) mesoscale and microscale weather systems/fields/processes embedded in unusually large and intense monsoon trough etc (Srinivasan 2013; Dube et al. 2014; Kotal et al. 2014; Joseph et al. 2015; Vellore et al. 2016; Houze et al. 2017; Priya et al. 2017). Several researchers emphasized the significant importance of moisture advection from the Arabian Sea and Bay of Bengal into the monsoon system, as well as

orographic lifting of moist airflows down a steep slope of the Western Himalaya. (Dube et al. 2014; Kotal et al. 2014; Singh et al. 2014; Joseph et al. 2015; Vellore et al. 2016; Ranalkar et al. 2016; Houze et al. 2017; Krishnamurti et al. 2017). Their conclusions are especially based upon, synoptic observations, satellite-radar output as well as numerical model simulations. Recently we have studied the heaviest monsoon rainstorm that occurred during 16-17 June 2013 over western slopes of Himalaya and concluded that, combined five factors: cool-low and warm-low regime contrast; squeezing of three different type of flows (deep warm-moist, cool-dry and warm-dry); orographic lifting; and pumping and suction effects produced unprecedented rains over Kedarnath range (Ranade and Singh 2021). In our earlier studies (Ranade and Singh 2014) concerning about the variations in spatio-temporal extreme rainfall fields over the Indian region, we observe that the point/local, short-duration extreme rain events (EREs) are embedded in large-scale, long-period intense heavy to very wet spells, and rainwater generated during the main monsoon wet period is highly correlated with the Asia-Pacific monsoon intensity. Many Numerical modelling studies have attempted to simulate as well as predict the Kedarnath event, and reported satisfactory results (Dube et al. 2014; Joseph et al. 2015; Shekhar et al. 2015; Cho et al. 2015; Chevuturi and Dimari 2016 and others).

Besides these, number of studies were undertaken keeping in view report of the International Disaster Database (<http://www.emdat.be>) which suggested a substantial increase in the extreme rain events (EREs) over western Himalayas in recent 30–40 years. Since 2010, numerous noticeable extreme events have been observed over Indian Himalayan region of Leh, Uttarakhand, Jammu and Kashmir and Himachal Pradesh, over subtropical Pakistan and over Nepal and China. Studies shows that, multiple visualizable factors operated in accord to produce extreme weather/rain events across subtropical Asia. Unprecedented interactions between deep westerly trough and cross-equatorial Indian Ocean south-westerlies as well as Pacific easterlies results in evolution of large and intense monsoon trough extending from Philippine through Indus basin. Arabian sea and Bay of Bengal provides the excessive moisture and numerous synoptic scales, mesoscale and microscale weather systems are evolved and interconnected in the anomalous monsoon trough along with topographical features results in increase in the severity of the events. Formation and intensification of troughs in the temperate westerlies is a short period phenomenon. Therefore, condensation and intense rainfall in subtropical mountainous terrain that involving confluence and convergence of huge airmasses of contrasting characteristics are short lived.

Various studies have documented the precipitation characteristics in the Himalayan region during rainstorm periods, while the detailed understanding of the evolution and intensification of the rain-producing weather systems at the boundary of the tropical (barotropic) and extratropical (baroclinic) regime is missing. It has been observed that the Himalayas exhibit distinct circulation dynamics between monsoonal and non-monsoonal weather systems, with significant seasonal variability. Even within the

monsoon period, rainstorm dynamics differ across early, established, and withdrawal phases, complicating the identification of common patterns for extreme rainfall event occurrences.

In this study, we propose a detailed systematic long-term analysis of various large-scale and isolated spatio-temporal extreme rain events during winter, pre-monsoon, monsoon and post-monsoon seasons of a year by considering three aspects of extremes viz. rainfall amount, area extent and duration over 3 states of the northwest Himalaya. Following are the objectives of the study in detail.

- To document broad features and unique characteristics of the large-scale and isolated heavy rainstorms/snowstorms across Northwest Himalaya
- To generate in-depth information about the location, shape, size, and intensity of the various rain-producing weather systems that are formed over the northwest Himalaya during different seasons of a year.
- To investigate the relationship among global atmospheric thermal structure and general and monsoonal circulation features and seasonal extremes over the NW Himalaya.
- To study the nature of mid/upper tropospheric tropical-extratropical interactions and different thermo-hydrodynamical processes causing isolated heavier rain/snow storms.

2. STUDY AREA AND DATASET USED:

The extreme rain events are identified by using by using $0.25^\circ \times 0.25^\circ$ Gridded daily rainfall observations. The atmospheric parameters like pressure (mslp), precipitable water (ppw), and temperature (T), geopotential height (Z) and wind (u and v) at 12 selected levels (1000–100 hPa) for the period 1979–2023 are taken from NCEP-CFSRV2 reanalysis (Saha et al. 2010, 2014). From arithmetic mean of the 6-hourly values, the daily dataset has been prepared.

Study Area: Northwest Himalaya

The Northwest Himalayan (NWH) region (fig 1), a climatically and topographically diverse zone of the Indian Himalayas, includes the states of Uttarakhand (UK), Himachal Pradesh (HP), and Jammu & Kashmir (J&K). This region spans a wide range of elevations—from low-lying foothills to high-altitude glaciated terrain—and plays a critical role in influencing the South Asian monsoon and western disturbances. Uttarakhand lies in the central part of the NWH, characterized by steep valleys and major river systems like the Ganga and Yamuna. It is prone to both monsoonal and post-monsoonal extreme rainfall events, often leading to flash floods and landslides. Himachal Pradesh occupies the midsection of the region, with complex terrain comprising the Lesser, Greater, and Trans-Himalayan ranges. It receives precipitation from both the southwest monsoon and winter western disturbances, and exhibits significant variability in seasonal rainfall. Jammu & Kashmir, the northernmost state in the study area, includes a vast

expanse of high-altitude terrain. It is strongly influenced by western disturbances, particularly during winter, and shows contrasting precipitation regimes across the Jammu plains, Kashmir Valley, and the cold desert of Ladakh. Together, these three states represent the broader hydrometeorological behavior of the NWH, making the region highly suitable for investigating long-term changes and extremes in rainfall under a changing climate.

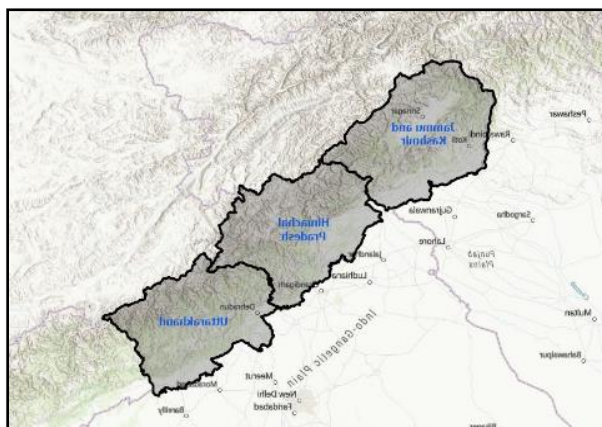


Fig 1. Study area: Northwest Himalaya

3. METHODOLOGY:

This study addresses a comprehensive long-term analysis of large-scale extreme rainfall events (LS-EREs) in the northwest Himalayas (NWH), covering Uttarakhand (UK), Himachal Pradesh (HP), and Jammu and Kashmir (J&K). It focuses on three key aspects of these extremes: rainfall magnitude, spatial extent, and event duration using high-resolution ($0.25^\circ \times 0.25^\circ$) gridded daily rainfall data. To explore the drivers of severe EREs, the study analyzes meteorological anomalies and physical processes using NCEP-CFSR-V2 reanalysis data of key atmospheric parameters such as temperature, pressure, geopotential height, wind fields, and absolute vorticity.

Inter-annual variations in area averages of annual and seasonal rainfall are studied using Mann-Kendall (MK) test for its trend detection. Spatial variation in long-term trends in grid-scale EREs across the NWH states are also studied by using MK test. An objective criterion has been developed to identify the 1- to 10-day large-scale long-period extreme rain events (LS-EREs) and small-scale spatio-temporal rain events (ST-EREs) for each year. The criteria use the daily mean rainfall (DMR) during a normal monsoon period as the threshold and the area under wet condition to determine areal extent. Anomalous meteorological conditions during LS-EREs are studied using composite analysis of top three EREs recorded during the study period. More details are given in figure 2.

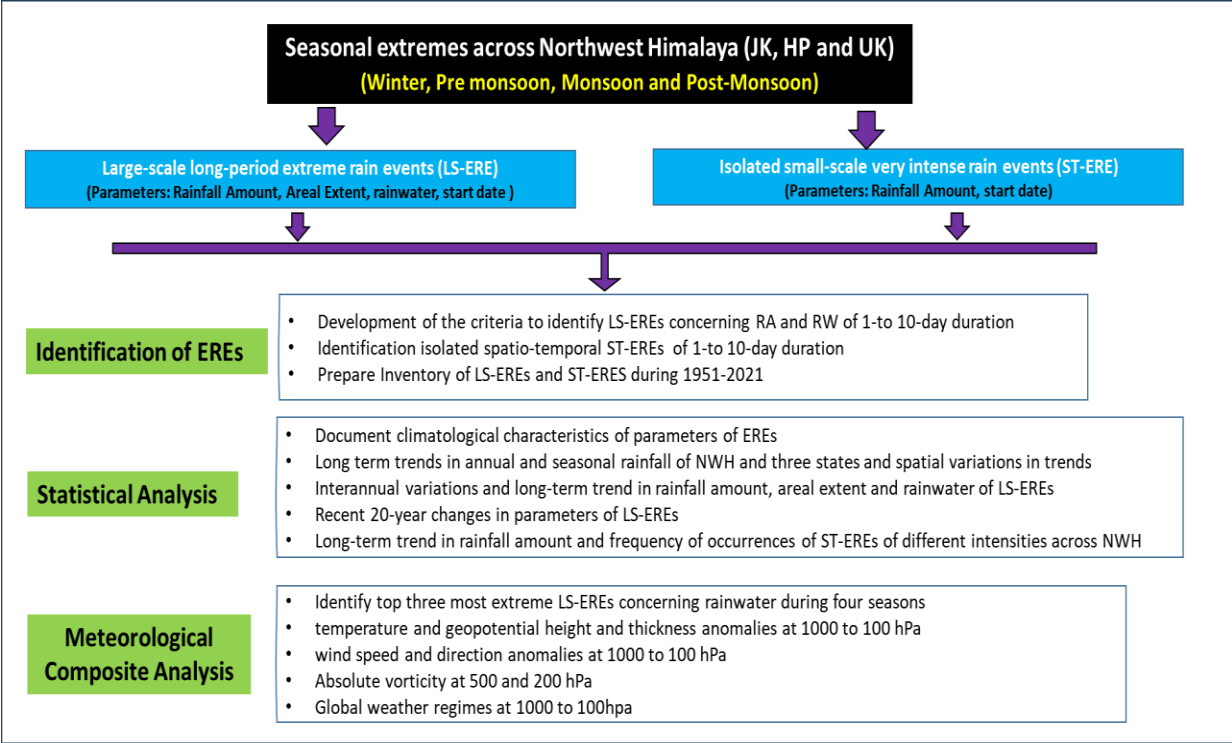


Fig 2. Methodology adopted for the analysis of Extreme rain events across NWH

4. ANALYSIS AND RESULTS:

4.1 ANNUAL AND SEASONAL RAINFALL CHARACTERISTICS ACROSS NW HIMALAYA

The analysis of annual and seasonal rainfall characteristics across the Northwest Himalaya (NWH) over the period 1951–2021 reveals significant spatial and temporal variations. Using daily gridded rainfall data, the study examines area-averaged rainfall for Uttarakhand (UK), Himachal Pradesh (HP), and Jammu & Kashmir (J&K) across different seasons: monsoon (JJAS), post-monsoon (OND), winter (JF), and pre-monsoon (MAM). The mean annual rainfall varies across the states, with UK receiving the highest (1444.7 mm), followed by HP (1244.85 mm) and J&K (1125.8 mm). Similarly, monsoonal rainfall is highest in UK (1096.5 mm), followed by HP (746.8 mm) and J&K (465 mm). However, the spatial distribution of rainfall across NWH (fig 3a) shows considerable variation, with annual rainfall ranging between 1281.4 mm to 4668.8 mm, while seasonal rainfall fluctuates significantly: winter (155.4–2311 mm), pre-monsoon (244.9–1504.0 mm), monsoon (453.8–4090 mm), and post-monsoon (240.3–1101.5 mm). Fig 3b shows spatial distribution in climatological annual and seasonal maximum rainfall across NWH during 1951-2021. The maximum annual rainfall varies between 1281.4-4668.8 mm across the three states, while seasonal maximum varies from 155.3-2311.6 mm during Winter; 244.8-1504.0 mm

during pre-monsoon; 453.7-4090.6 mm during monsoon; and 240.3-1101.5 mm during post-monsoon season.

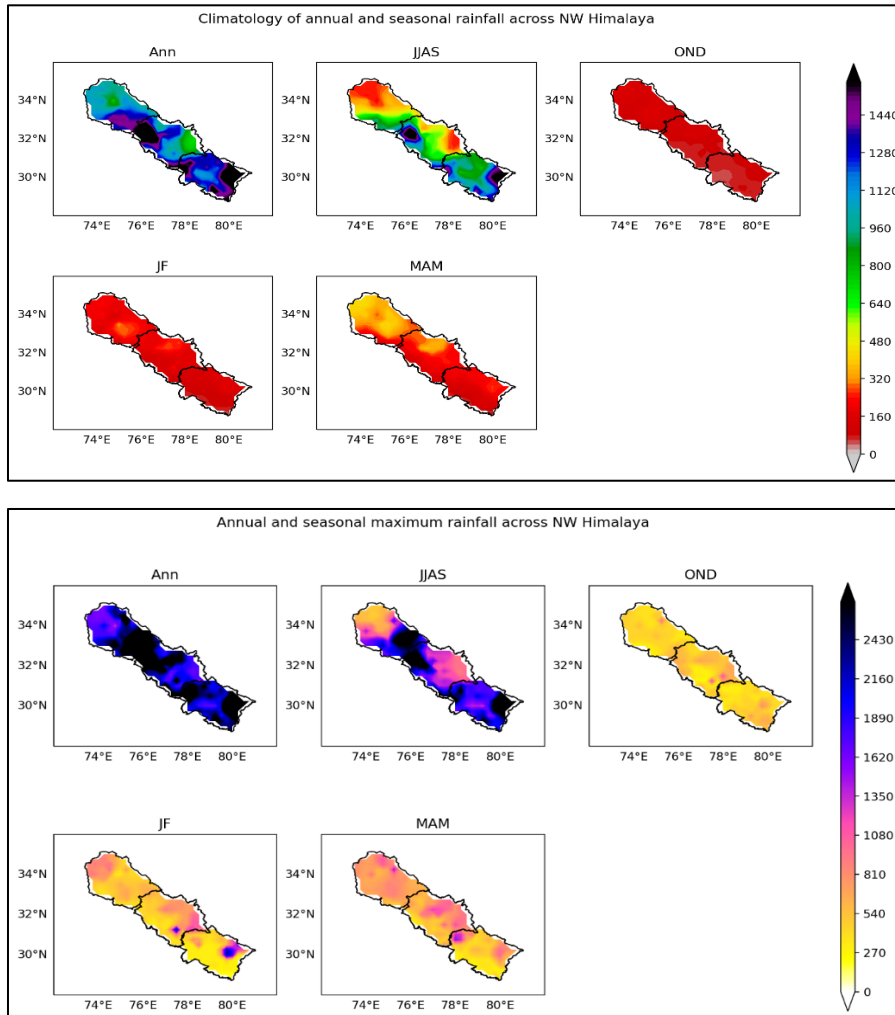
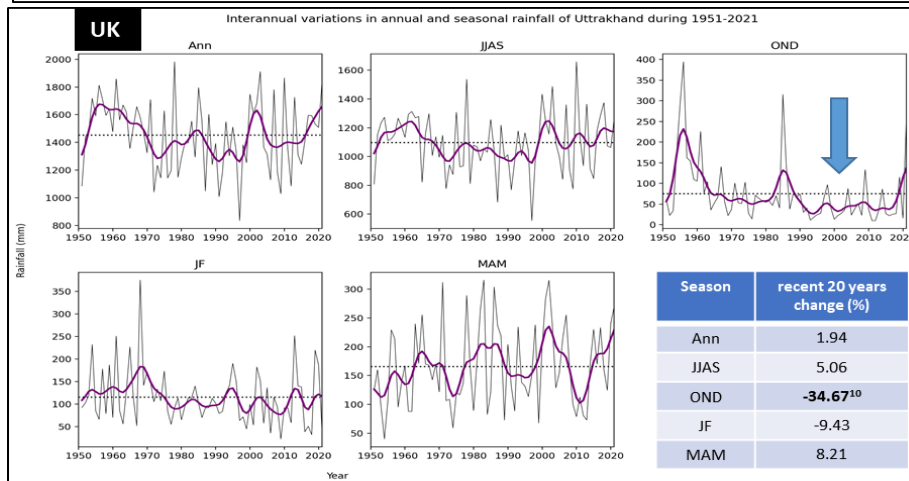
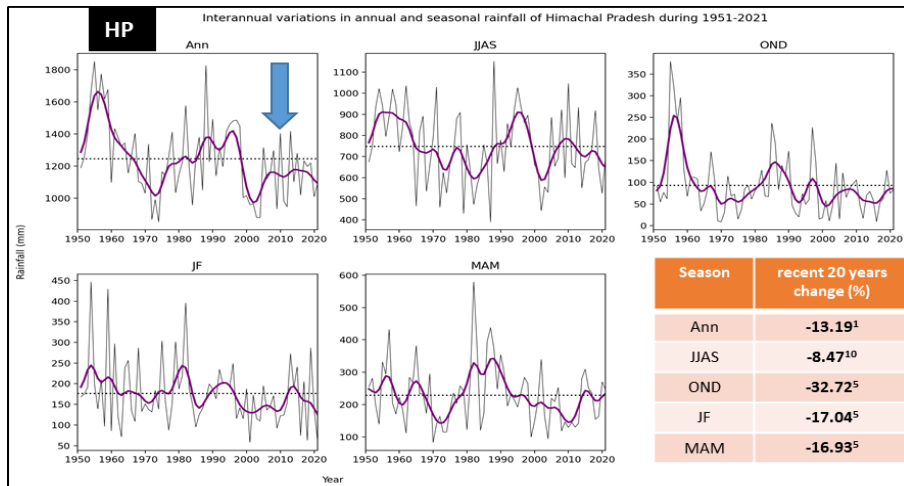
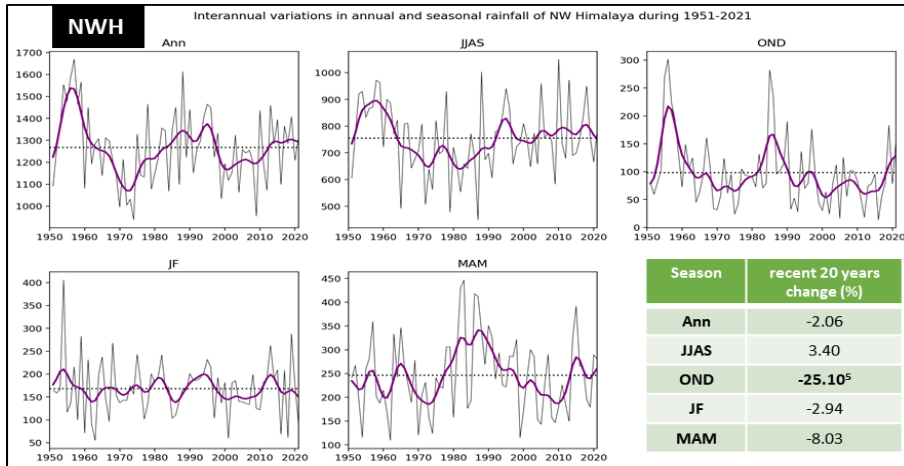


Fig3. Spatial distribution of climatological mean (top) and maximum (bottom) of annual and seasonal rainfall across NWH

4.1.1 LONG-TERM TREND AND RECENT YEAR CHANGES

To detect long-term trends, the Mann-Kendall test is applied to the area-averaged annual and seasonal rainfall series. Figure 4 shows interannual variations and recent 20-year changes in annual and seasonal rainfall of NWH, UK, HP and J&K states. No significant long-term trends are noticed in annual and seasonal rainfall of NWH, however, OND rainfall shows significant decrease of -25% in recent 20 years compare to preceding period. Changes in annual and other seasonal rainfall are statistically non-significant. In Uttarakhand, no significant long-term trend is observed in annual and monsoonal rainfall, but OND rainfall shows a significant long-term decline (1951-2021), with a 35% decrease in the last 20 years (2001-2021). In Himachal Pradesh, a significant long-term decline in annual rainfall is detected, with a 13% decrease in the last 20 years. Additionally, monsoon rainfall declined by ~8.5%, OND by

~33%, winter (JF) by 17%, and pre-monsoon (MAM) by ~17%. Conversely, J&K exhibits a significant long-term increasing trend in winter (JF) rainfall, while other seasonal and annual rainfall series remain homogeneous and random. In recent years, monsoonal rainfall in J&K has increased by ~18% compared to the preceding period.



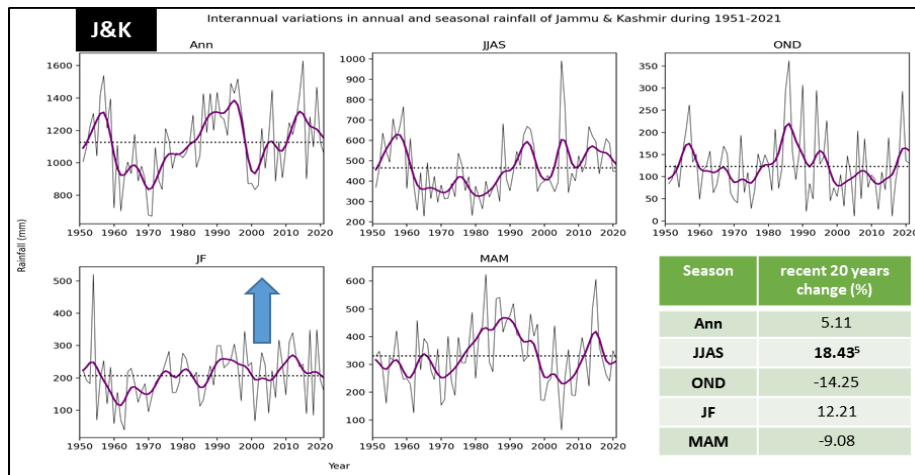


Fig 4. Interannual variations and recent 20 year changes in annual and seasonal rainfall across NWH and three states

Spatial trend analysis shown in figure 5 reveals a significant decline in annual rainfall across most parts of HP and some regions in UK, while J&K shows a significant increase. Monsoonal rainfall is increasing over J&K and highly elevated areas of HP and UK, whereas low-lying regions experience a decline. Post-monsoon rainfall in UK has significantly decreased, whereas winter rainfall in J&K has notably increased. These findings underscore the diverse hydro-climatic changes across the NWH region, with important implications for water resource management, agriculture, and disaster risk mitigation.

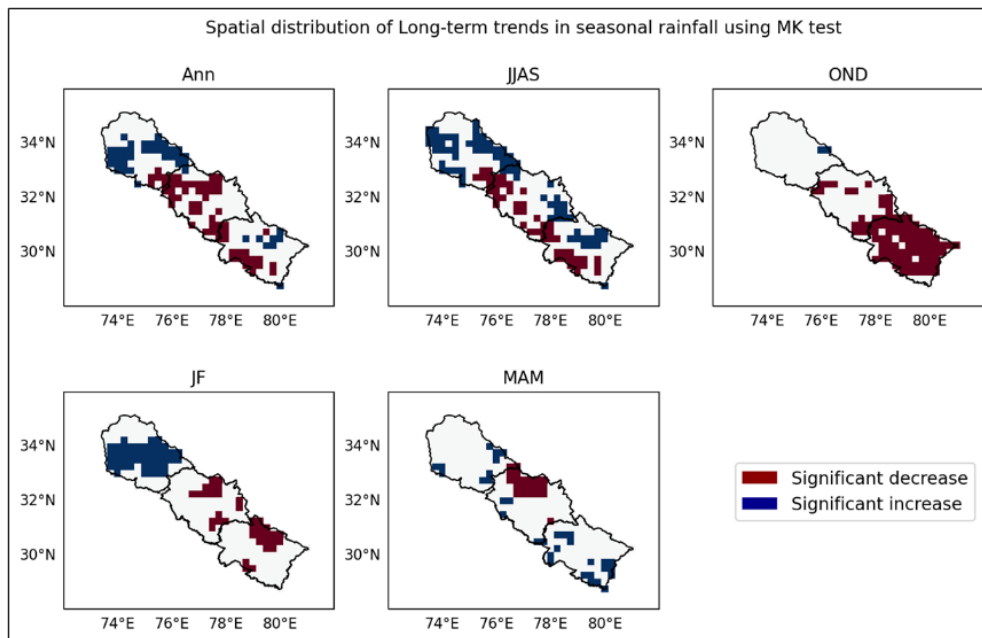


Fig 5. Spatial variations in Long-term trend in annual and seasonal rainfall during 1951-2021

4.2 IDENTIFICATION OF LARGE-SCALE EXTREMES CONCERNING RAINFALL AMOUNT (ERE-RA) AND RAINWATER (ERE-RW)

The 1-to 10-day duration large-scale extreme rain event are intended to quantify the severity of persisting intense rains over a particular area. An objective criterion has been developed to identify 1- to 10-day large-scale EREs concerning rainfall amount and rainwater (rainfall multiply by the area) for each year during 1951-2021 over NWH and three states. On daily basis, each grid is identified under wet condition if actual rainfall exceeds the daily mean monsoon rainfall (DMR) of the particular grid. The DMR is the daily mean rainfall during normal monsoon period over the grid taken as the threshold. On the grid scale, the DMR varies between less than 2mm/day to more than 18mm/day across NWH (fig 6). During 1951-2021 the highest DMR is observed at station Dharamshala, Kangra district, Himachal Pradesh.

The rainfall amount of ERE-RA refers to annual maximum cumulative rainfall of wet grids for the duration 1- to 10-days. The rainwater of ERE-RW refers to the total accumulated rainwater of wet grids for the duration of 1- to 10 days. The procedure has been applied for each year of the period 1951–2021 to get the sequence of extreme rain events for 1–day to 10-days durations. The other parameters of the extremes like areal extent (AE) of ERE-RA and date of start of ERE-RA and ERE-RW are also documented.

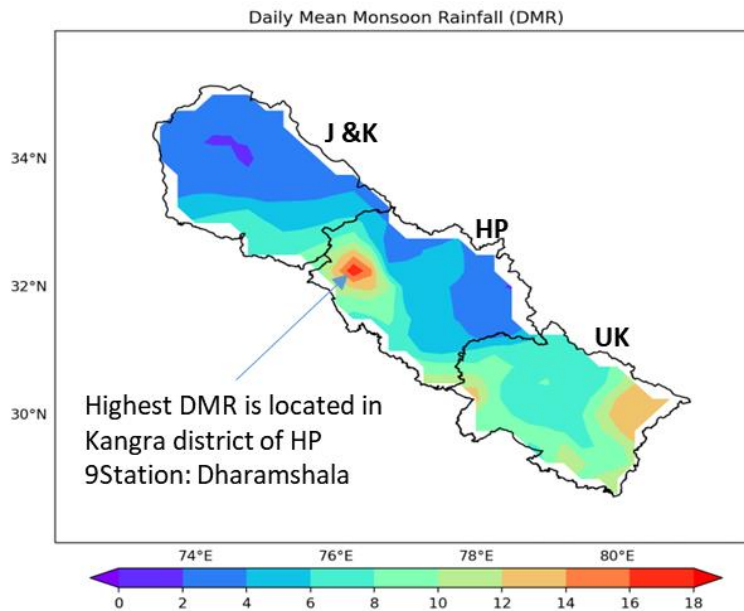


Fig 6 Spatial distribution of daily mean monsoon rainfall across NWH

Table 1 shows climatological characteristics of parameters of LS-EREs of 1- to 10-days duration while table 2 shows those for three states in NWH. Normally the rainfall amount of ERE-RA over NWH increases from 58.04 mm (± 20.77) to 203.36mm (± 36.54) for 10-days duration. Over UK it increases from 71.50mm (± 31.70) to 148.14mm (± 54.54); HP 57.05mm (± 18.12) to 206.84mm (± 42.47) and J&K 58.58mm (± 29.63) to 175.22mm (± 46.26) respectively. The areal extent does not show much variations over the duration for

all the three states. The percentage areal under wet condition is ~70% over UK and J&K and ~57% over HP.

Table 1 Climatological characteristics of parameters of 1 to 10-day large-scale ERE-RA and ERE-RW over NWH

Duration of EREs	ERE-RA		ERE-RW
	Rainfall Amount (\pm SD) in mm	Areal-Extent (in percent)	Rainwater (in bcm)
1-day	58.04(\pm 20.77)	45.69(\pm 30.6)	5.97(\pm 1.76)
2-day	88.94 (\pm 25.27)	50.33(\pm 31.69)	9.79(\pm 2.98)
3-day	110.85 (\pm 33.13)	50.80(\pm 30.75)	12.25(\pm 3.68)
4-day	128.82 (\pm 34.14)	47.59(\pm 30.27)	14.03(\pm 4.09)
5-day	141.72 (\pm 33.64)	47.90(\pm 30.27)	15.65(\pm 4.44)
6-day	154.34 (\pm 35.31)	47.48(\pm 30.45)	17.04(\pm 4.53)
7-day	165.75 (\pm 35.16)	46.32(\pm 30.50)	18.32(\pm 4.66)
8-day	178.38 (\pm 37.45)	46.57(\pm 28.38)	19.65(\pm 4.72)
9-day	190.55(\pm 35.98)	45.70(\pm 26.99)	20.88(\pm 4.86)
10-day	203.36 (\pm 36.54)	45.87(\pm 27.63)	22.18(\pm 5.04)

Seasonal/ Month-wise distribution of 1-day large-scale extreme event occurrences during 1951-2021 shows that, the year-wise large-scale ERE-RA and ERE-RW mostly occurred during monsoon season. Out of total ERE-RA occurrences, about 69-85% events occur during monsoon, 7-13% occur in post-monsoon, 3-11% occur during pre-monsoon and 4-11% during winter season across NWH. Similar distribution can be seen for the occurrences of ERE-RW as well (fig 7). Even though the monsoonal contribution in the frequency of EREs is more, surprisingly in some years, the severity of non-monsoonal extremes surpassed the monsoon extremes especially over HP and J&K.

Table 2. Climatological characteristics (mean and SD) parameters of 1 to 10-day large-scale ERE-RA and ERE-RW over three states of NWH

Duration of EREs	Uttarakhand			Himachal Pradesh			Jammu & Kashmir		
	ERE-RA		ERE-RW	ERE-RA		ERE-RW	ERE-RA		ERE-RW
	RA (mm)	AE (%age)	RW (bcm)	RA (mm)	AE (%age)	RW (bcm)	RA (mm)	AE (%age)	RW (bcm)
1-day	71.50 (±31.70)	66.65 (±33.87)	2.80 (±1.30)	57.05 (±18.12)	54.18 (±38.49)	2.29 (±0.83)	58.58 (±29.63)	70.01 (±34.87)	3.01 (±1.24)
2-day	109.67 (±40.19)	73.56 (±32.29)	4.52 (±1.75)	86.88 (±24.97)	66.79 (±35.41)	3.81 (±1.41)	90.80 (±29.62)	73.93 (±34.15)	4.73 (±1.96)
3-day	134.73 (±47.16)	72.92 (±33.05)	5.60 (±2.09)	109.96 (±35.46)	60.36 (±37.28)	4.77 (±1.80)	110.18 (±38.12)	75.21 (±33.77)	5.78 (±2.47)
4-day	154.87 (±48.91)	71.99 (±33.34)	6.39 (±2.26)	129.50 (±40.83)	56.46 (±37.70)	5.40 (±2.04)	123.18 (±41.41)	74.31 (±34.08)	6.36 (±2.71)
5-day	169.79 (±49.45)	70.19 (±33.62)	7.13 (±2.38)	142.34 (±42.87)	54.20 (±37.35)	5.94 (±2.22)	134.64 (±44.12)	72.03 (±34.64)	6.86 (±2.93)
6-day	185.62 (±48.96)	67.68 (±33.76)	7.74 (±2.44)	154.43 (±43.06)	58.15 (±36.60)	6.41 (±2.28)	142.03 (±45.26)	70.74 (±35.07)	7.19 (±3.01)
7-day	203.13 (±51.85)	67.82 (±33.37)	8.37 (±2.52)	169.52 (±35.55)	54.47 (±34.55)	6.88 (±2.30)	149.94 (±44.42)	67.19 (±36.61)	7.49 (±3.0)
8-day	220.80 (±54.85)	66.20 (±35.31)	9.07 (±2.62)	181.83 (±41.61)	52.89 (±34.15)	7.32 (±2.29)	158.67 (±44.08)	65.65 (±36.47)	7.82 (±3.01)
9-day	235.93 (±55.33)	71.16 (±31.78)	9.73 (±2.70)	194.11 (±41.95)	51.94 (±33.49)	7.72 (±2.31)	166.77 (±44.54)	65.91 (±35.65)	8.20 (±3.04)
10-day	148.14 (±54.54)	70.83 (±31.80)	10.34 (±2.74)	206.84 (±42.47)	55.81 (±33.67)	8.19 (±2.37)	175.22 (±46.26)	66.24 (±34.99)	8.52 (±3.09)

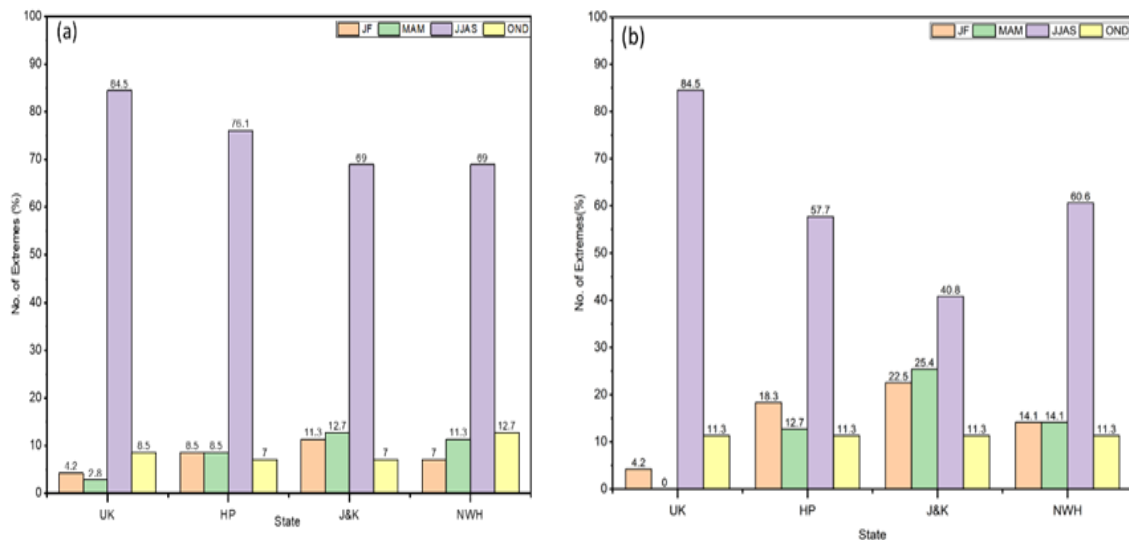


Fig 7. Seasonal distribution of year-wise most severe 1-day large-scale ERE-RA and ERE-RW occurrences

4.3 LONG-TERM TRENDS AND RECENT CHANGES IN PARAMETERS OF LARGE-SCALE EXTREMES

Inter-annual variations in parameters of LS-EREs are studied and the significance of trend is tested using Mann-Kendall test. Results show that, RA of 8- to 10-day ERE-RA of NWH show significant decreasing trend. Over UK, RA does not show any significant trend however, over HP, it shows significant decrease for 3- to 10-days duration events (fig 8). Over NWH, AE of 2-day ERE-RA shows significant increasing trend. Over HP no significant trend is observed in AE of ERE-RA however over J&K, significant increasing trend is observed in AE of 1- to 6-day ERE-RA.

During 1951-2021, over NWH, rainwater of 1-day ERE-RW shows significant increasing trend. Over UK, no significant trend is observed, however over significant increase is observed in RW for 1-2-day ERE-RW of J&K, and significant decrease is observed over HP for 5-10 day ERE-RW (Figure 9).

Table 3 shows recent 20 years changes in parameters of 1- to 10-day LS-EREs over NWH and three states. In last 20 years no significant change is observed in RA of ERE-RA over NWH, however significant increase is seen for RA of 1-to 5-day ERE-RA over UK and 1-day ERE-RA over J&K. Significant decrease in RA is seen for 2 to 5-day ERE-RA over HP. The AE of 1- to 3-day ERE-RA is significantly increased over NWH in recent 20 years. No significant change is observed over UK and HP, but significant decrease is seen for 1-day and 4- to 5-day ERE-RA over J&K. Rainwater of 1- day ERE-RW is significantly increased over NWH and J&K. Significant increase is also seen for 1-to 5-day ERE-RW over UK but significant decrease is observed for 4- to 5-day ERE-RW of HP.

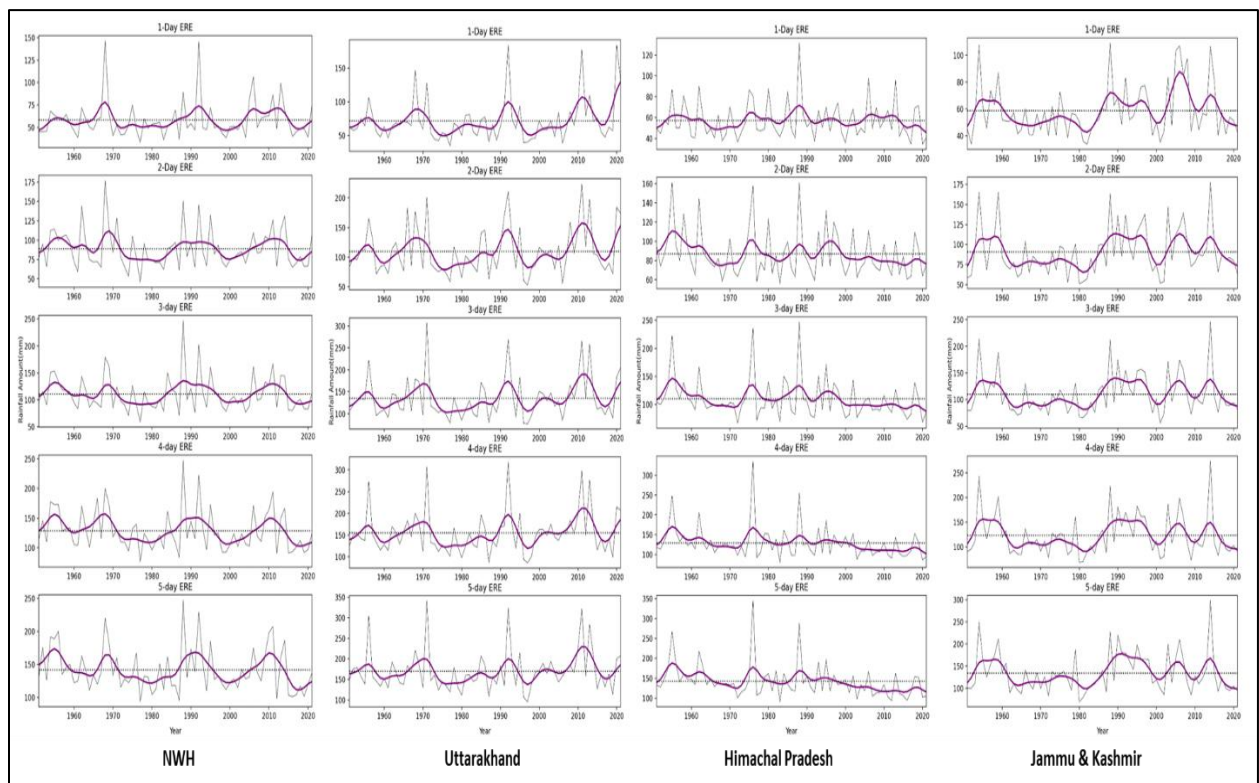


Fig.8 Interannual variations in rainfall amount of large-scale ERE-RA over NWH and three states

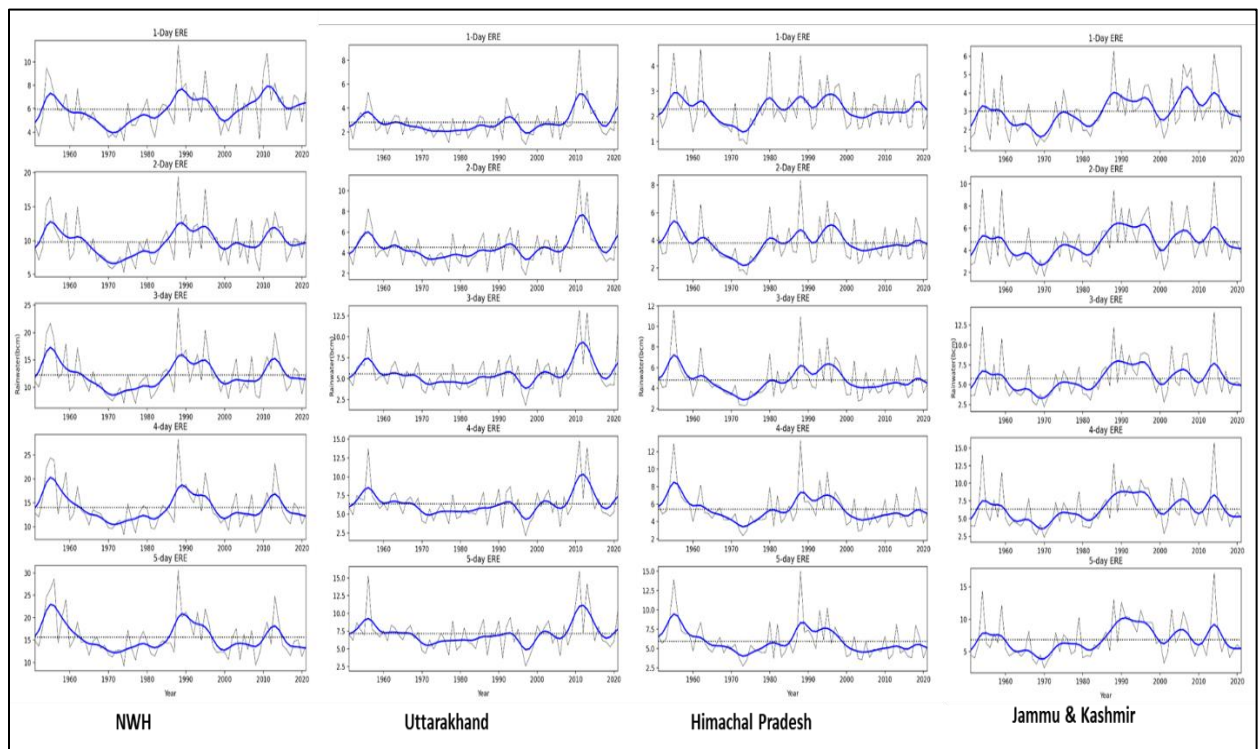


Fig.9 Interannual variations in rainwater of large-scale ERE-RW over NWH and three states

Table 3. percentage change in recent 20 years (2001-2021) compare to preceding (1951-2000) period in parameters of large-scale EREs of 1- to 10-day durations

Duration of EREs	NWH			UK			HP			J&K		
	ERE-RA		ERE-RW	ERE-RA		ERE-RW	ERE-RA		ERE-RW	ERE-RA		ERE-RW
parameters	RA (%)	AE (%)	RW (%)	RA (%)	AE (%)	RW (%)	RA (%)	AE (%)	RW (%)	RA (%)	AE (%)	RW (%)
1-day	7.57	28.24 ¹⁰	15.94 ⁵	23.22 ⁵	15.61	34.52 ¹	-1.44	0.71	-4.74	16.28 ⁵	21.41 ⁵	23.30 ⁵
2-day	-0.15	31.14 ⁵	3.46	14.76 ¹⁰	9.24	25.95 ¹	-10.27 ¹⁰	-0.72	-6.74	7.91	11.27	12.54
3-day	-3.17	43.76 ¹	0.95	12.56 ¹⁰	14.95	25.29 ¹	-14.23 ⁵	8.98	-9.88	6.10	13.80	9.66
4-day	-5.83	20.23	-3.37	13.20 ⁵	0.14	21.68 ⁵	-17.64 ⁵	-0.47	-16.19 ⁵	0.56	20.54 ⁵	7.77
5-day	-3.79	14.92	-6.88	10.72 ¹⁰	0.61	19.82 ⁵	-18.87 ¹	10.89	-19.91 ⁵	-0.25	23.36 ⁵	6.44
6-day	-4.58	-2.53	-7.62	8.82	-1.13	17.47 ⁵	-19.01 ¹	13.88	-19.80 ⁵	-0.24	19.91 ⁵	5.53
7-day	-5.30	1.92	-7.24	7.74	3.75	16.88 ⁵	-18.15 ¹	-8.74	-17.78 ⁵	-1.27	19.56 ¹⁰	4.66
8-day	-5.62	2.31	-6.31	6.84	-1.98	16.70 ⁵	-18.84 ¹	-12.25	-16.32 ⁵	0.08	6.71	7.09
9-day	-5.80	4.56	-6.01	5.28	9.59	16.02 ⁵	-20.28 ¹	-11.75	-15.23 ⁵	-1.19	12.76	9.33
10-day	-5.33	-5.17	-4.95	3.47	8.01	14.28 ⁵	-19.96 ¹	7.91	-14.97 ⁵	-0.47	11.82	23.30 ⁵

In order to study the relationship of rainfall and duration of the EREs, the analysis has extended for 25-day durations. The cumulative rainfall amount/rainwater are plotted against the duration of EREs. The mean RA/RW of all EREs are also plotted against their respective standard deviation. It has been observed that, the seven selected values (highest observed, mean plus 2sd {standard deviation}, mean plus 1sd, mean minus 1sd, mean minus 2sd, mean minus 2sd. and lowest observed values; y-axis) from the distribution of cumulative rainfall amount of ERE-RA and rainwater of ERE-RW for 1- to 25-day duration increases following a quadratic relationship with the duration (x-axis) (figure10). The coefficients of the equation $Y=A+ Bx+ Cx^2$ are also shown in figure 10. The standard deviation (SD) which is the absolute major of variability also seen increases linearly with the increase in mean maximum rainfall amount/rainwater.

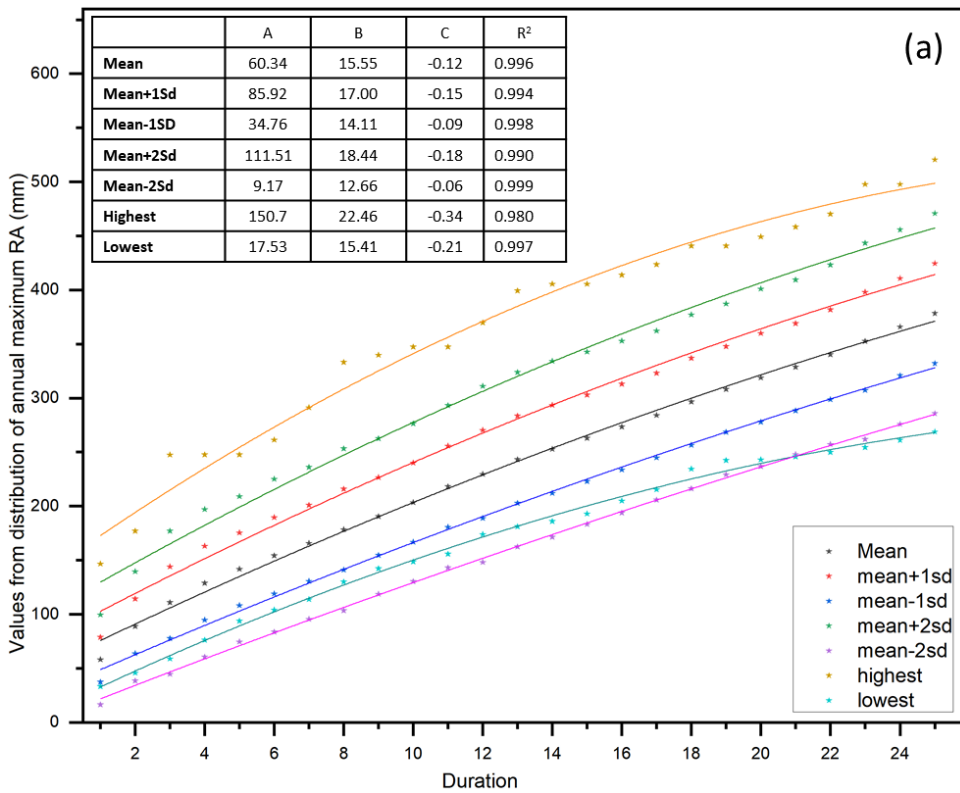
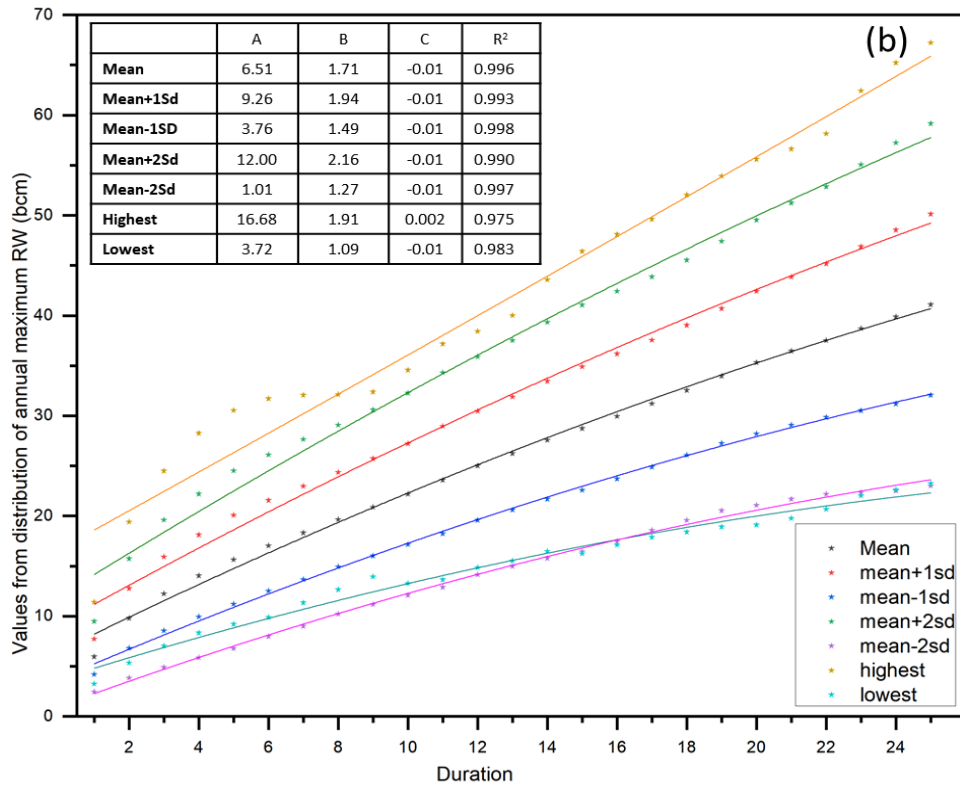


Fig 10. Relationship of Rainfall Amount (a) and Rainwater (b) with the duration of 1- to 25-day EREs over NWH

4.4. IDENTIFICATION AND CHARACTERISTICS OF SMALL-SCALE ISOLATED SPATIO-TEMPORAL EXTREMES (ST-ERES):

Small-scale isolated extreme rain events exhibit large inter-annual spatial variability. To understand characteristics of these extremes an elaborate analysis of temporal and spatial variability of 0.25 deg grid scale EREs of 1- to 10-day duration has been carried out. The annual maximum rainfall series on grid scale for one day has been prepared during 1951-2021 by selecting year-wise highest rainfall amount for a particular grid. Similarly annual maximum rainfall series for 2 to 10-day duration are also prepared. Figure 11 shows spatial distribution of mean RA of ST-EREs and that for most extreme ST-EREs of 1- to 10-day durations. The mean rainfall of 1-day ST-ERE spatially varies from 50.3mm to 168.9mm across NWH states. For 10-day ST-ERE, the rainfall varies from 121.23mm to 528.15mm. The spatial variation of highest experienced rainfall during the study period shows that, for 1-day ST-EREs, most extreme rainfall varies between 106mm and 762.9mm, while for 10-day most extreme ST-EREs, the rainfall varies between 263mm to 1423mm.

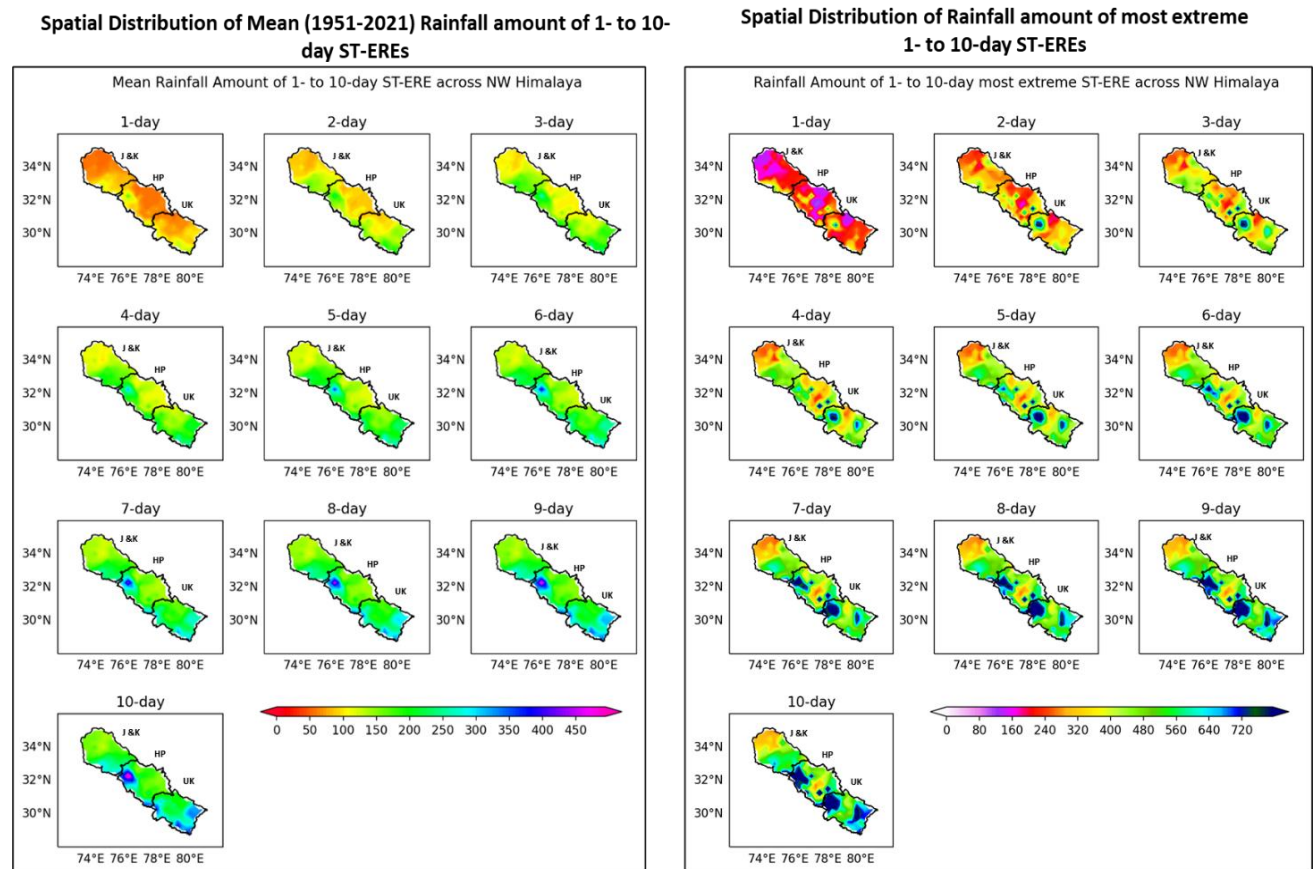


Fig 11. Spatial variation in mean rainfall amount of 1-to 10-day ST-EREs and that for most Extreme ST-EREs

Mean frequency of occurrences of 1-day ST-EREs of different intensities are calculated and shown in figure 12. Left panel shows spatial distribution of annual mean frequency of 1-day EREs of intensity

varies from 1*DMR to 10*DMR, while right panel shows that during monsoon across NWH. Results show that, low intensity ST-EREs are widespread across NWH with higher frequency over J&K. While, Most of the severe extreme rain events (rainfall >8 DMR) are less frequent and mostly occur in northern J&K and high-altitude southern regions of HP and UK.

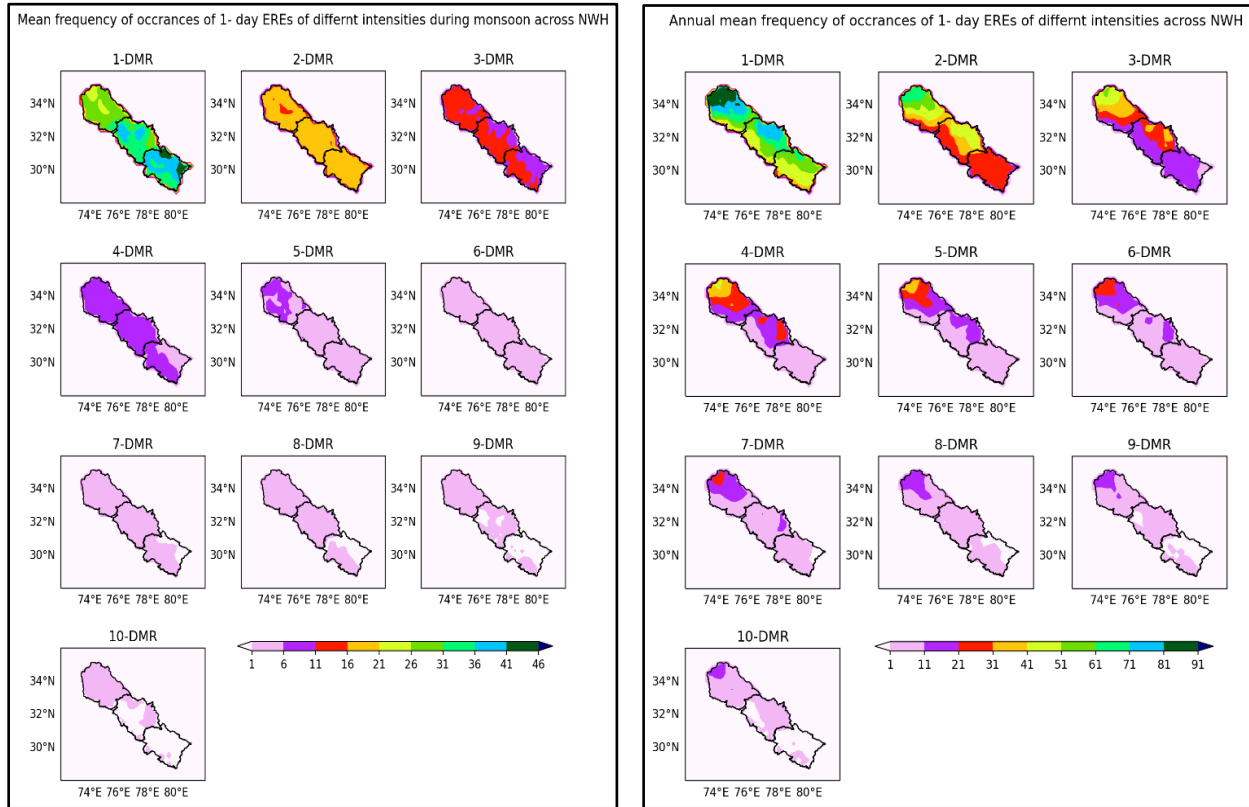


Fig 12. Annual and monsoonal mean frequency of occurrences of 1-day Extremes of different intensities

4.5 TREND ANALYSIS OF RAINFALL AND FREQUENCY OF OCCURRENCES OF ST-ERES:

The spatial trend analysis using Mann-Kendal test show that the rainfall of 1-day ST-ERE shows significant increase over major part of J&K and high elevated part of UK. However, most part of HP and some part of UK with lower elevation shows significant decrease in rainfall amount of long-period extremes ranging more than 2 days. This indicates that, short-duration ST-EREs in high-altitude areas are intensified and that of prolonged duration are reduced in lower regions. Spatially coherent significant long-term trend is not seen in rainfall amount of 1- to 10-day ST-ERE across NWH (fig 13).

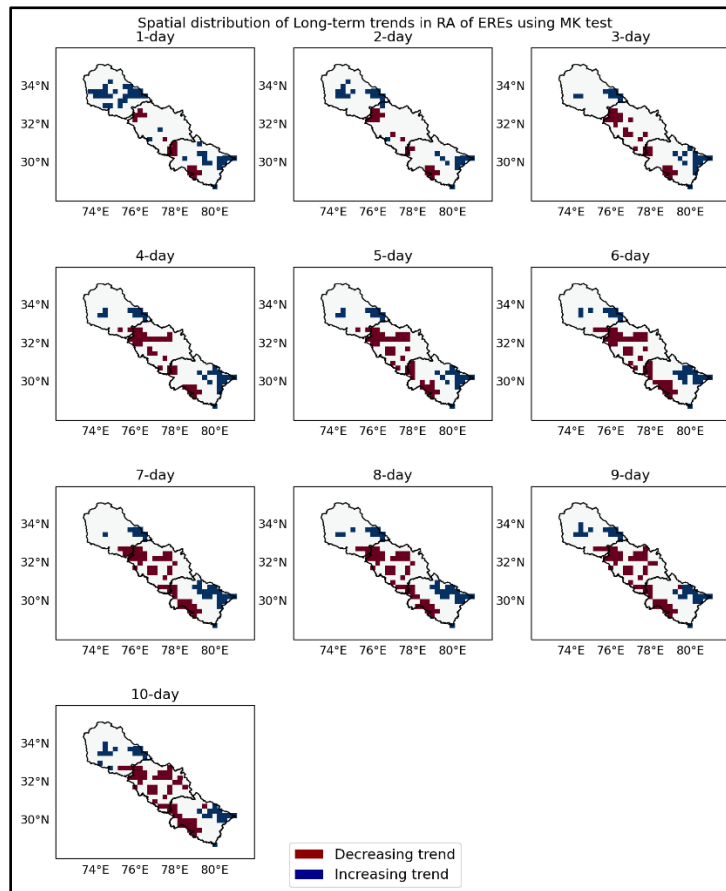


Fig 13. spatial distribution of long-term trend in rainfall of 1-to 10-day ST-EREs during 1951-2021

Spatial distribution of trend values for the frequency of occurrences of ST-EREs of different intensity annually and during monsoon are shown in fig 14. Significant increase in ERE frequency observed over high altitude regions, especially in J&K and parts of UK. This is more pronounced for high intensity rainfall category ($RF > 8\text{DMR}$). While some low altitude regions of HP and UK exhibit significant decrease in ERE occurrences particularly more moderate intensity events. During Monsoon, the low intensity events (2-4 DMR) are significantly decreased in some low-altitude areas of HP and southern UK, while significant increases in high-altitude regions of J&K and parts of UK. Moderate to High intensity EREs (6-12 DMR) are increased in high-altitude regions in scattered manner over northern J&K and parts of northern J&K. These trends reveal a shift towards more frequent extreme rainfall events in high-altitude regions, especially in J&K and northern UK, while moderate-intensity rainfall events are decreasing in lower altitude regions, including HP and southern UK.

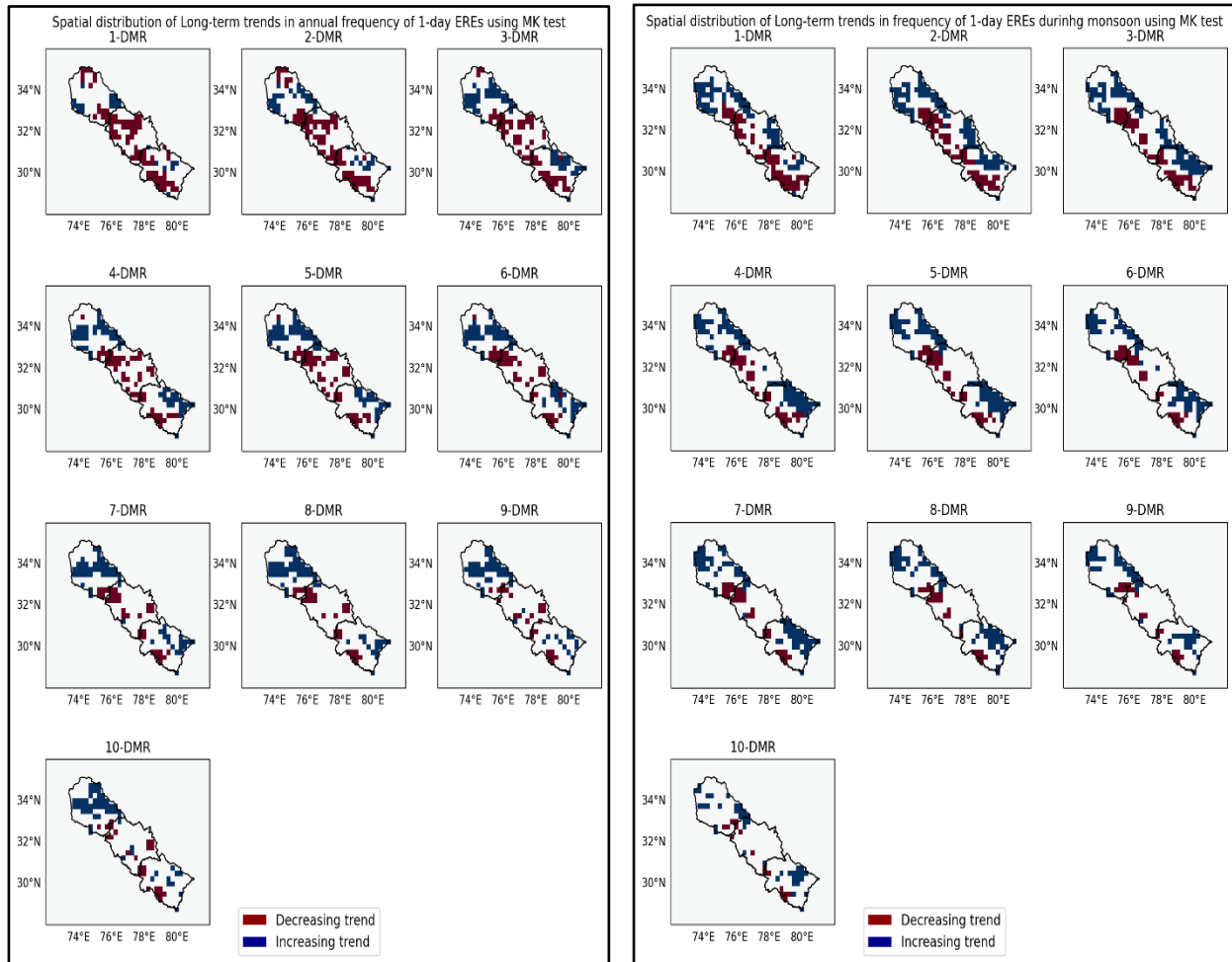


Fig 14. (a) Spatial distribution of long-term trends in annual frequency of 1-day ST-EREs of different intensities; and (b) that for monsoon season

4.6 ELEVATION DEPENDANT OCCURRENCES OF ST-ERES

In order to understand the relationship of occurrences of EREs with the elevation of Himalaya, we have superimposed the extreme rainfall intensity with the elevation data extracted from DEM. Fig 15 shows the mean rainfall intensity of 1- to 10-day ST-EREs and the elevation above 300m meters. It has been seen that, Most of the severe ST-EREs of the duration 1- to 3-days are observed to occur below 3000m of elevation and mostly in the states of Himachal Pradesh and Uttaranchal.

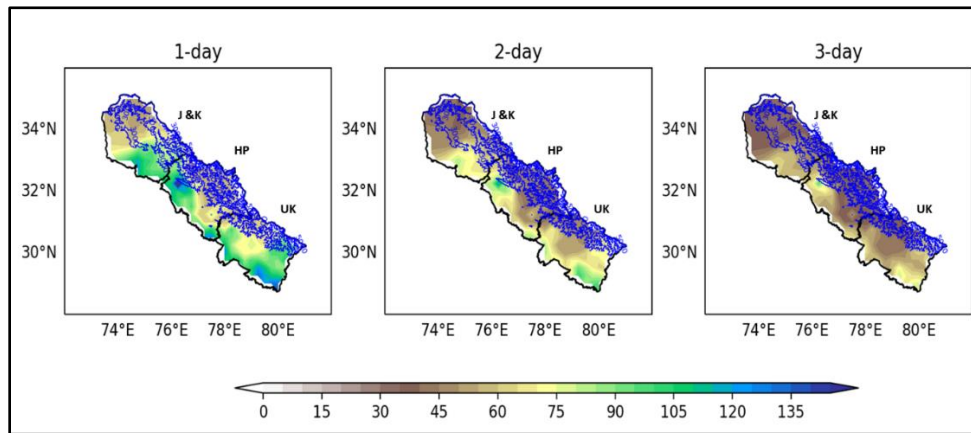


Fig 15. Mean rainfall intensity of 1- to 3-day ST-EREs and elevation (above 3000m).

4.7 WEATHER SYSTEMS ASSOCIATED WITH RAIN/SNOW OVER NW HIMALAYA

The Himalayas experience rain from a variety of weather systems, changing with the seasons. Each system has its own dominant season, spatial focus (eastern vs western Himalayas), and rainfall characteristics (steady, convective, extreme). The unique orography, proximity to both tropical and mid-latitude circulation systems, and complex terrain make this region prone to diverse rain-producing systems. Rainfall in this region is crucial for glacier health, agriculture, and water resources, but also contributes to natural hazards such as floods, landslides, and cloudbursts. Understanding seasonal rainfall mechanisms is vital for improving forecasts and disaster preparedness. The northwestern Himalayas are characterized by steep terrain ranging from 300 m to over 7000 m in elevation. This region lies at the intersection of tropical monsoon systems and mid-latitude westerlies. Orographic lifting plays a dominant role in enhancing rainfall, and the seasonality of rainfall sources adds further complexity. Dominant influences include the Indian Summer Monsoon (ISM), Western Disturbances (WDs), and local convective processes.

- **Winter season:** Western Disturbances (WDs) that originating from the Mediterranean and Caspian regions, are mid-latitude synoptic-scale systems that bring widespread stratiform precipitation plus snowfall to the western Himalayas. These systems transport moisture and interact with the orography to produce stratiform rain and snowfall. Occasionally, deep WDs lead to localized cloudbursts and flash floods, especially during rain-on-snow events.
- **Pre-Monsoon Season:** Pre-monsoon thunderstorms forms when solar heating intensifies, and local instability develop. They are convective in nature. When residual WDs interact with surface heating, isolated heavy rains can occur. This period may also witness river floods due to simultaneous snowmelt and rainfall.
- **Monsoon season:** Monsoon season experiences three types of weather systems, monsoon lows/depressions, monsoon trough oscillations and cloudbursts. During monsoon low-pressure systems and depressions that originate in the Bay of Bengal and move northwestward, producing

widespread rain upon interacting with Himalayan terrain. Orographic lifting and high atmospheric moisture lead to heavy and sometimes extreme rainfall. The monsoon trough occasionally shifts northward, resulting in intense rainfall along the Himalayan foothills. Break-monsoon phases can also cause significant rain accumulation. The cloudbursts are localized, high-intensity rainfall events (>100 mm/hr as per IMD criteria), often occurring due to orographic lifting of moisture-laden air during peak monsoon months. Cloudbursts are responsible for many catastrophic flash floods and landslides in Himachal Pradesh, Uttarakhand, and parts of Kashmir.

- **Post-Monsoon Season:** As the monsoon withdraws, remnant low-pressure systems interact with early WDs, occasionally triggering light to moderate rainfall. This season helps recharge soil moisture before winter.

Rare systems such as tropical cyclone remnants (e.g., from the Bay of Bengal) can bring rain to the region in post-monsoon months. Tibetan anticyclone interactions and intrusions of mid-latitude troughs may lead to off-season rain events.

WDs significantly contribute to snowpack and water availability, while monsoon systems are the primary source of rainfall. Cloudbursts, although rare, result in disproportionate damage due to their high intensity. Thunderstorms and rain-on-snow events can lead to landslides and rapid flooding. Thus, the Northwestern Himalayas experience complex, seasonally varying rainfall systems driven by both tropical and mid-latitude dynamics. Understanding these systems is essential for disaster risk reduction, water management, and climate adaptation. Integrated research combining observations, reanalysis data, and high-resolution models is critical for anticipating changes in rain-producing mechanisms in this fragile mountainous region.

4.8 COMPOSITE METEOROLOGICAL ANALYSIS OF MOST EXTREME LS-ERES IN DIFFERENT SEASONS.

Most severe 1-day large-scale extreme rain events concerning rainwater are identified for each season (DJF: winter, MAM: pre-monsoon, JJAS: monsoon and ON: post-monsoon) during 1951-2021. Composites charts of temperature, geopotential, wind and relative vorticity at 12 isobaric levels for top three severe extremes are prepared and analysed in details.

4.8.1 MOST EXTREME LS-ERES DURING WINTER

The top three most extreme LS-ERES during winter happened on 09.02.2010, 19.02.2003 and 30.12.1990. The rainfall distribution, rainwater collected and the duration of extreme on these days is shown in figure 16. One dominated by spatial spread, another by intensity core, and the third by duration and stratiform nature—highlighting the dynamic variability of Western Disturbance-induced precipitation systems in the region. 9th Feb 20210 event shows wide spread and well distributed heavy rainfall that likely be linked to strong WD system causing prolonged precipitation over larger area. In 19th Feb 2003 event, though the

volume is slightly less than the 2010 event, the spatial peak is much higher, indicating a localized but intense convective core, surrounded by stratiform rain. It suggests a hybrid WD system with embedded mesoscale convection. 30 Dec 1990 event is a classic widespread winter WD event, characterized by sustained but moderate precipitation rates. It reflects strong stratiform precipitation driven by mid-latitude moisture intrusions and orographic lifting over the Himalayan foothills.

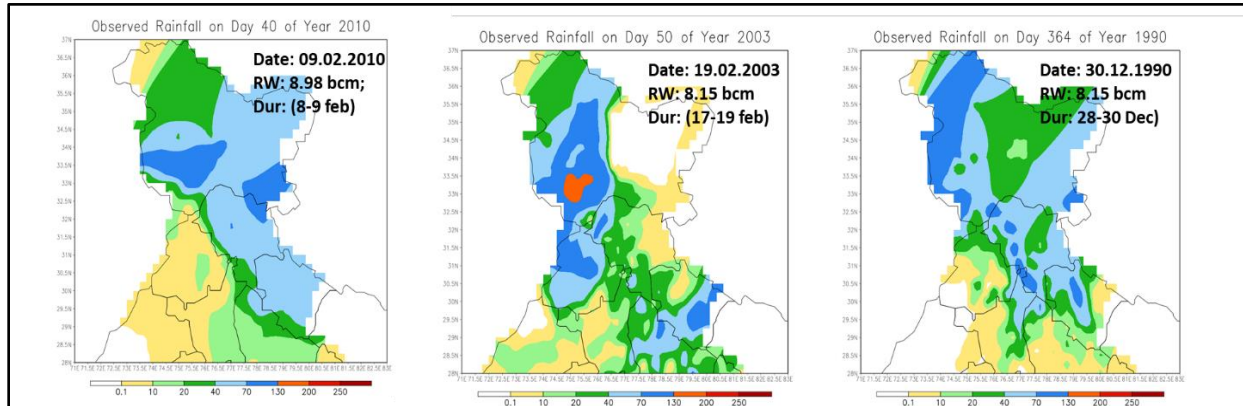


Fig 16. Rainfall field during most severe LS-EREs during winter season of 1951-2023

Composites of temperature Anomalies at 850 hpa, and 200hpa prior to, during and after the occurrences of winter extremes (fig 17) reveals that, during winter-time ERE days, strong cold anomalies develop over Eastern Europe and Central Asia, while warm anomalies appear over Northern Africa, the Arabian Sea, and the Bay of Bengal, creating a sharp temperature gradient at lower level. Intrusion of cold air mass from high latitude interacts with the advection of moist warm air that strengthens the unstable baroclinic zone. Cold anomalies aloft signifies the upper level trough enhancing the vertical motion that supports extreme uplift and precipitation. The combination of low-level warm-cold temperature contrasts (850 hPa) and upper-level cooling (200 hPa) creates a favourable environment for strong uplift, instability, and heavy rainfall during LS-EREs.

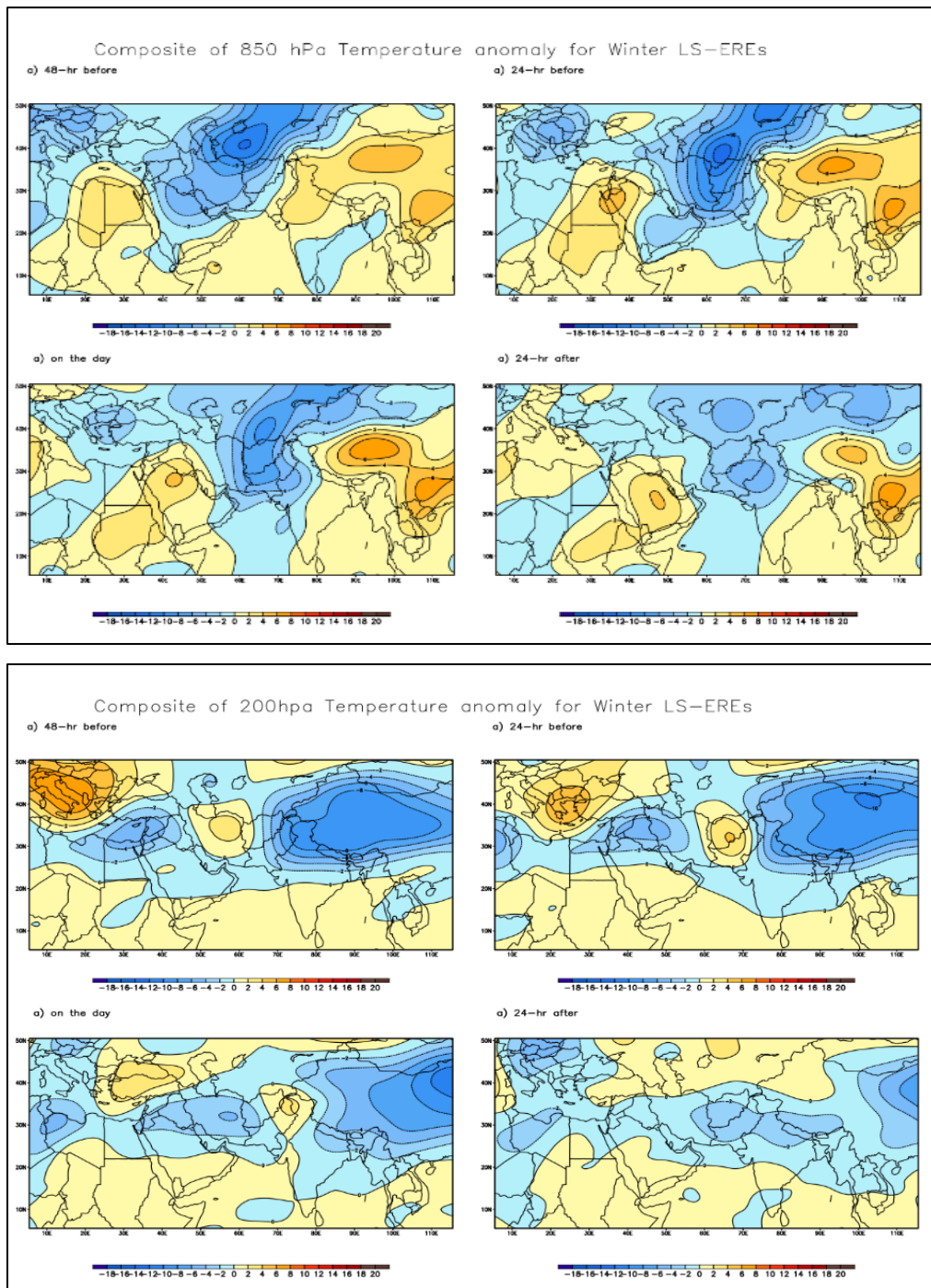


Fig 17. Composites of temperature Anomalies at 850 hpa, and 200hpa prior to, during and after the occurrences of LS-ERE over NWH during Winter

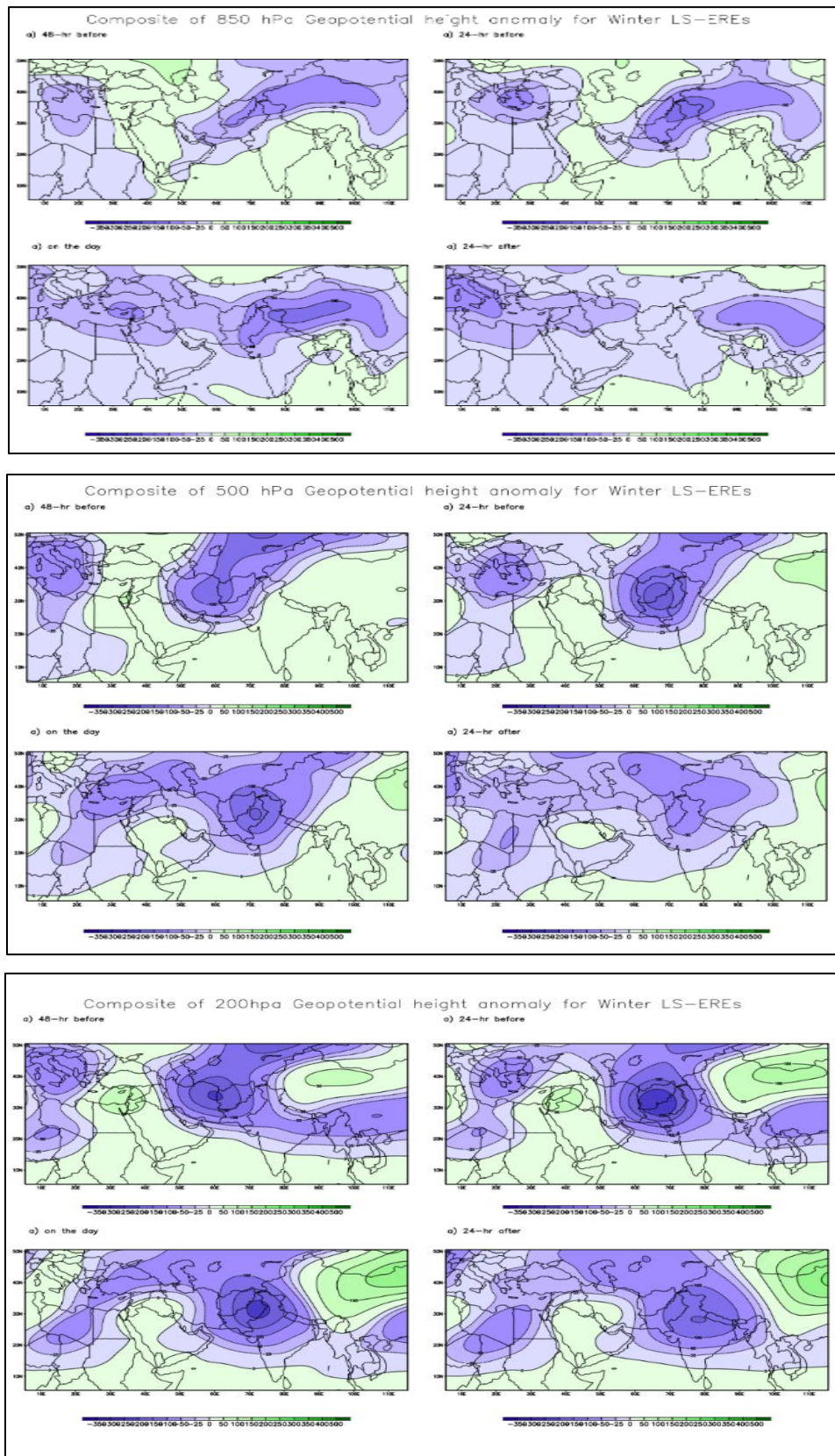


Fig 18 . Composites of geopotential height Anomalies at 850 hpa, 500hPa and 200hpa prior to, during and after the occurrences of LS-ERE over NWP during Winter

Figure 18 shows composites of geopotential height anomalies at 850 hpa, 500hPa and 200hpa prior to, during and after the occurrences of LS-ERE over NWH during Winter. Negative anomalies at lower level dominate Central Asia and the Middle East, indicating a low-pressure system strengthening near the surface. This supports cold air intrusion from the north. A pronounced negative anomaly at 500 hpa indicates the deepening of the mid-level trough. Strong negative anomaly at upper level represents upper-level trough and interaction with subtropical or polar jet stream before increasing the divergence aloft. A deepening mid-level trough and upper-level divergence strengthen the low-pressure system, facilitating cold air advection. The alignment of low-level low pressure, a mid-level trough, and upper-level divergence forms a vertically stacked system, indicating a well-structured western disturbance. Baroclinic instability and vertical motion drive extreme rainfall and cold events.

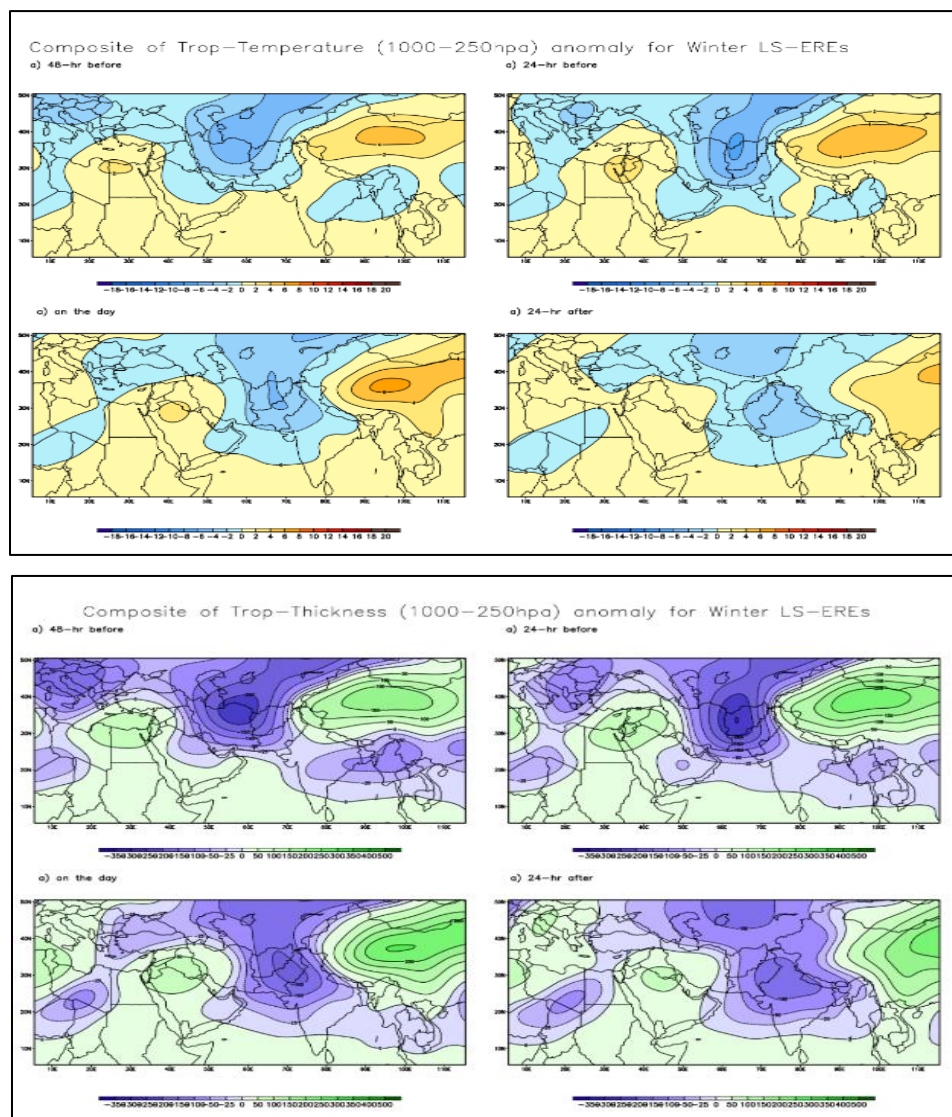


Fig 19. Composites of tropospheric temperature and thickness anomalies prior to, during and after the occurrences of LS-ERE over NWH during Winter

The cold tropospheric temperature anomaly and reduced thickness indicate the advection of cold air masses by WDs, which destabilize the atmosphere over the Himalayas (figure 19). This leads to strong vertical motions and facilitates precipitation. The combination of cold air advection, steepened temperature gradients, reduced tropospheric thickness, and orographic lifting creates conditions favorable for heavy precipitation or snowfall, characteristic of wintertime extreme events in the region.

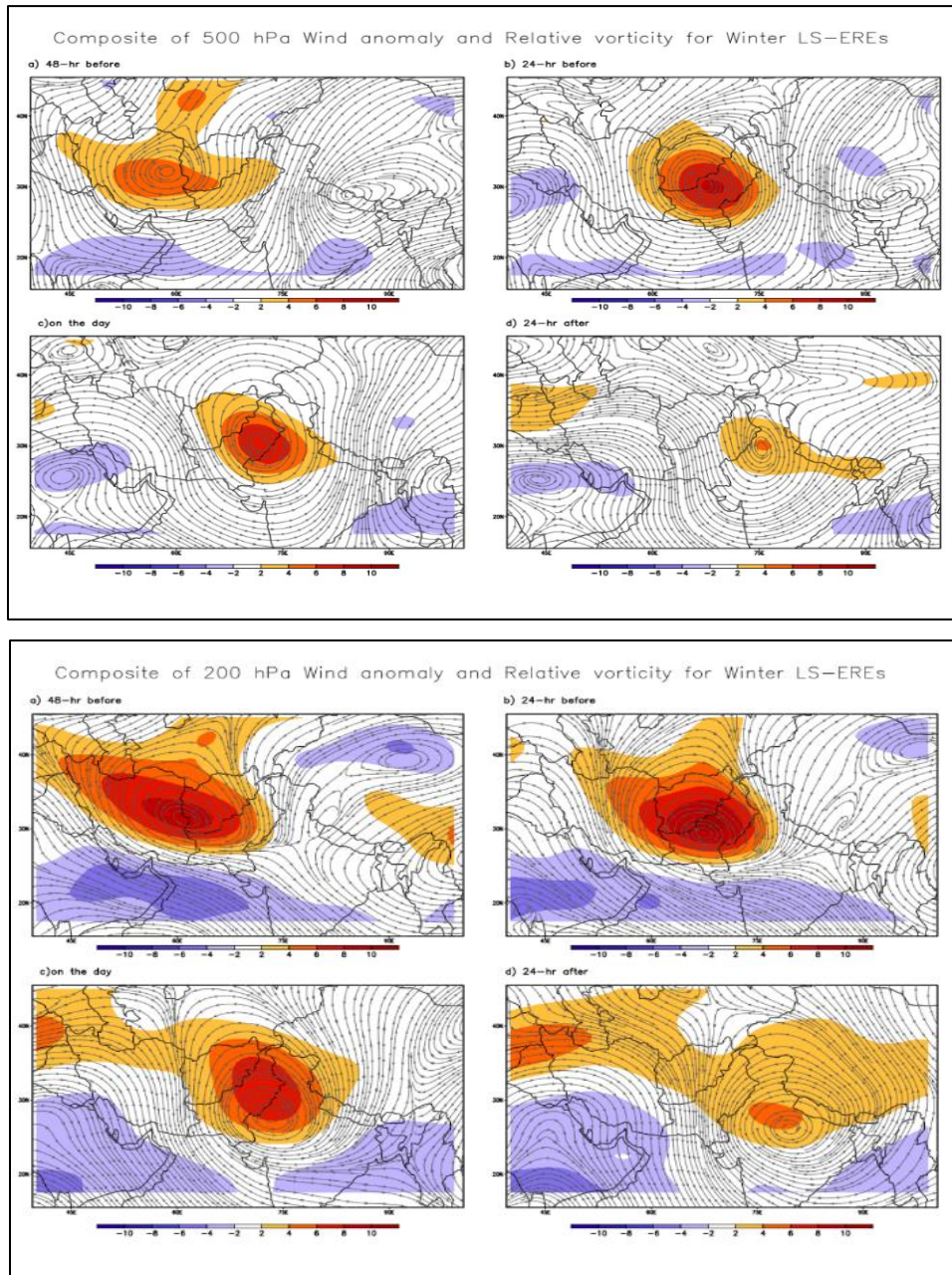


Fig 20. Composites of wind anomalies and relative vorticity at 500hPa and 200hPa prior to, during and after the occurrences of LS-ERE over NWH during winter

Strong positive vorticity with pronounced cyclonic anomaly is centred over central Asia indicating early development of mid-tropospheric trough 48 hours before (figure 20). The vorticity increased and cyclonic anomaly intensified while approaching the day of event. Strong upper level anomaly and positive vorticity align with surface. Negative anticyclonic anomaly in northwest direction indicate the interaction with jet stream. The interaction of mid-level cyclonic activity and upper-level divergence, indicate the propagation of WDs crucial for the intensification of winter LS-EREs. Both mid- and upper-level systems exhibit a clear progression, with peak intensity on the event day and subsequent dissipation within 24 hours

LS-EREs are also analysed using equatorially/globally conditioned meteorological analysis technique. The technique is developed (Ranade and Singh 2019) to study the evolution of monsoon and comprehend changes in global atmospheric thermal and circulation during extreme rain events. It has been observed that, monsoon circulation evolves in association with spreading and intensification of equatorial atmospheric thermal condition (warmest-thickest troposphere and lowest pressure), vertical circulation structure (lower tropospheric confluence/convergence and upper tropospheric diffluence/divergence), and highest precipitable water. The technique comprises global weather charts of equatorially, globally conditioned atmospheric parameters like mean sea level pressure (EC-mslp), precipitation water (EC-ppw), level-wise (1000–100hPa) atmospheric temperature (EC-T_{level}), geopotential height (EC-Z_{level}), wind (GC-W_{level}). By combining the equatorially conditioned parameters, the technique classifies the weather systems into four types of global weather regimes (GWRs).

1. Warm Low regime (WL): $EC-T > 0$ and $EC-Z < 0$
2. Cool-low regime (CL): $EC-T < 0$ and $EC-Z < 0$
3. Warm-high regime (WH): $EC-T > 0$ and $EC-Z > 0$
4. Cool-high regime (CH): $EC-T < 0$ and $EC-Z > 0$

Level wise distribution of the GWRs, streamlines and GC-W_{level} for full depth of the atmosphere would be helpful to visually gauge intensity of different weather systems (including location and intensity of jet stream) as well as to differentiate two or more systems of the same basic nature (lows or highs) in different climatic zones. This analysis provides adequate insight into the 3D structure of the monsoon circulation, area under monsoon condition, intensity and depth of monsoon circulation, start and end of seasonal rains and extreme rain events.

Composites of global weather regimes and streamlines at different atmospheric levels are prepared. Fig 21 shows normal GWR during winter as well GWRs composites of winter extremes at 850hPa, 600hPa, 400hpa and 200hPa. In normal winter conditions, cool-low anomalies dominated through most tropospheric layers, characteristic stable zonal westerlies, and limited vertical interactions conducive to extreme weather. At 850 hpa, normal cool-high regime (barotropic) is replaced by cool-low baroclinic regimes, dominated throughout the atmosphere. It indicates that slow rising motion in the lower level and intense divergence in the upper level. Strong cyclonic circulation associated with western disturbance is distinctly evident over

NW India and Pakistan. Mid troposphere is still dominated by the cool-low regime indicating continuity of lower-level cool anomalies extending upward. Streamlines show clearly enhanced troughing and cyclonic circulation just northwest of the Himalayas, indicating robust dynamic support for precipitation from mid-tropospheric levels. In upper troposphere, stronger and more widespread Cool-Low anomalies dominate extensively over the NW Himalayan region at upper levels, creating significantly amplified upper-level troughing.

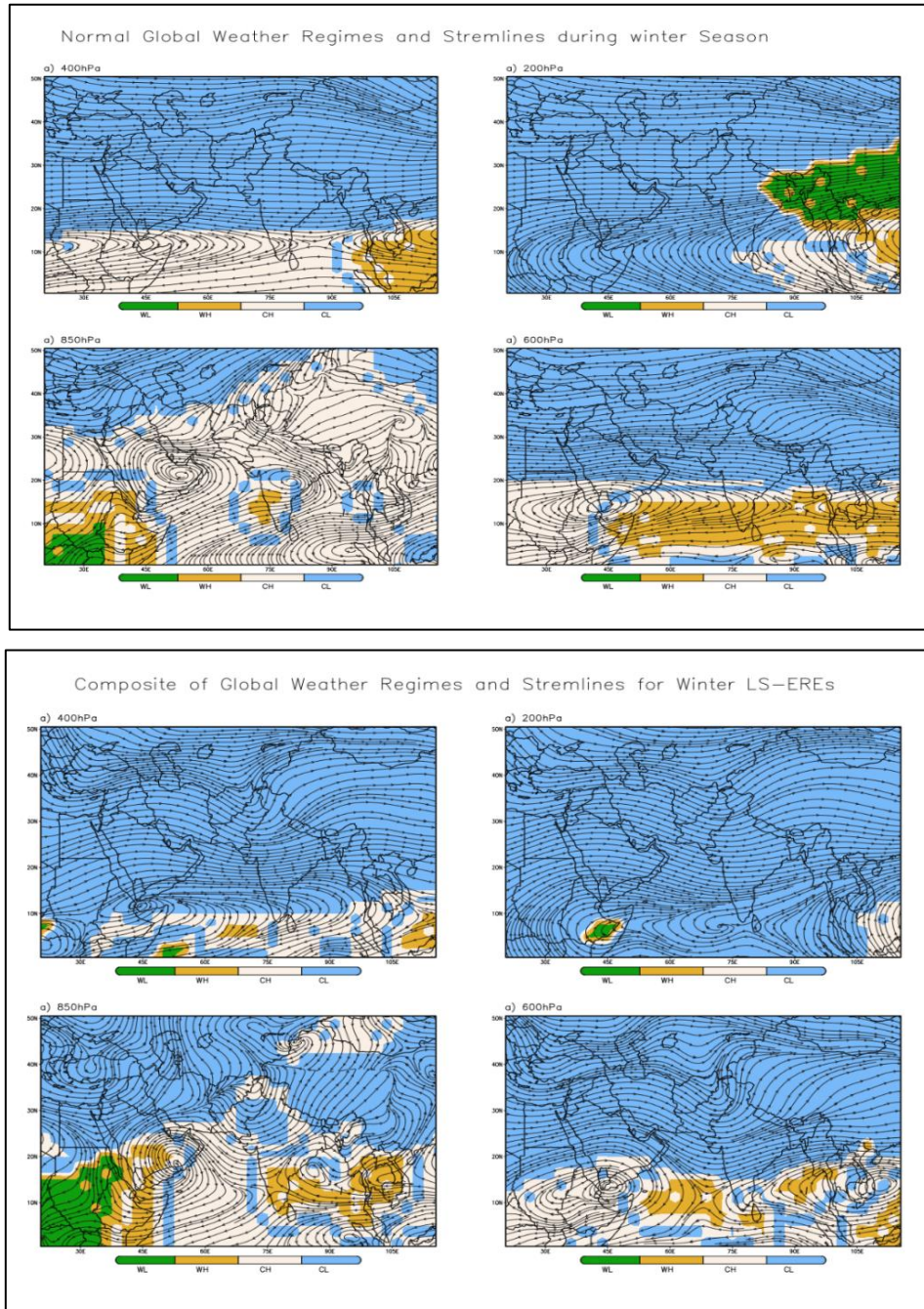


Fig 21 Normal Global weather regimes at 850 hPa, 600hPa, 400hPa and 200hpa during winter and composites for the occurrences of LS-EREs over NWH during winter

At 200 hPa, prominent wavy patterns indicate intensified troughing directly aligned over NW Himalaya, crucial for strong upper-tropospheric divergence and vertical lifting mechanisms. Upper-level streamlines depict distinct divergence patterns above the NW Himalayan region, suggesting highly favorable dynamical conditions for heavy precipitation.

Thus, Winter LS-EREs over NW Himalaya are primarily driven by Cool-Low anomalies extending vertically from lower to upper troposphere, combined with strong upper-tropospheric troughing and divergence. This vertical alignment of cool-low conditions enhances baroclinic instability, particularly favored in winter due to pronounced temperature gradients associated with mid-latitude westerlies. Strong upper-level divergence directly above robust cyclonic lower-level circulation (western disturbances) generates intense upward vertical motion, despite the absence of prominent low-level warming. This is dynamically consistent with classic winter extreme events driven by strong upper-level jet dynamics, mid-latitude troughs, and frontal activities, rather than tropical-type convection.

4.8.2 MOST EXTREME LS-EREs DURING MONSOON

The top three most extreme LS-EREs during winter happened on 25.09.1998, 16.08.2011 and 05.09.1995. The rainfall distribution, rainwater collected and the duration of extreme on these days is shown in figure 22. The 25th Sept 1988 event is late monsoon event, still a large swath of rainfall exceeding 100 mm/day spans the central and southern portions of the NWH. Extremely intense core (>250 mm/day) is observed over the southwestern region (dark red patches), likely due to a mesoscale convective system or monsoon depression remnant. The high RW value suggests high areal spread and intensity, leading to significant runoff and potential flood risk. 16th Aug 2022 event occurred during peak monsoon season. The rainfall pattern is more compact but contains a very intense rainfall core (>250 mm/day) in the southeastern part of the NWH. Widespread heavy rainfall (40–130 mm/day) surrounds the core, suggesting a combination of deep convection and moisture-laden large-scale ascent. Likely associated with monsoon low-pressure system or break-monsoon convection triggering localized flooding. In 05 Sept 1995 event, multiple patches of very heavy rainfall (>200 mm/day) are scattered, especially in the central and eastern basin sectors. The pattern reflects a mix of localized convective bursts and stratiform rain, possibly associated with an eastward-moving monsoon depression or orographically triggered convection. Despite slightly lower total volume than the first two events, the intensity is very high and could have led to short-duration flash flooding. These three monsoon LS-EREs display varying spatial and temporal structures but share the common traits of high intensity, deep vertical moisture support, and large basin-wide rainfall volumes.

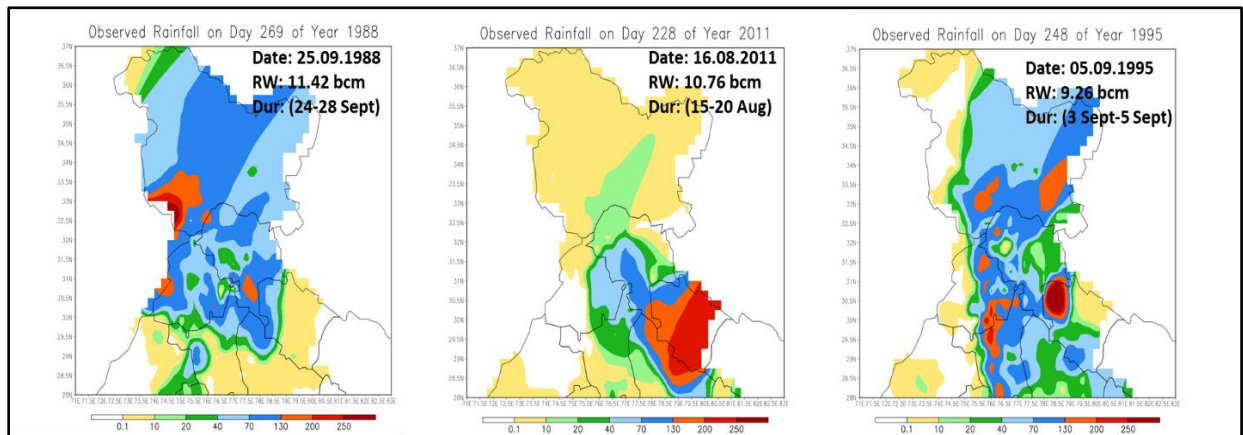


Fig 22. Rainfall field during most severe LS-EREs during monsoon season of 1951-2023

Composites of temperature Anomalies at 850 hpa, and 200hpa prior to, during and after the occurrences of monsoon extremes are shown in fig 23. At 850 hPa, 48 and 24 hours before the event, notable cold anomalies dominate over Central and South Asia, including the NWH region, indicating pre-event cooling at the lower level. On the day of the event, the cold anomaly remains widespread and intensifies, signifying strong cold advection and enhanced convective activity. 24 hours after the event, the cold anomaly weakens, but its persistence suggests sustained cooling due to continuous rain-induced temperature drops. At 200 hpa, 48 and 24 hours before the event, warm anomalies prevail in most regions, with weak cold anomalies at some locations, suggesting upper-level stability initially. On the day of the event, a stronger cooling trend emerges at the upper level, reinforcing upper-level trough development, which enhances vertical motion and instability. 24 hours after the event, the upper-level temperature anomaly starts to normalize, indicating the dissipation of the system. Thus during monsoon, strong cooling at lower level suggests presence of cloud cover and enhanced moisture convergence and upper-level cooling indicates the development of a trough and increased instability. This pattern of strong baroclinic instability, upper-level divergence, and cold advection contribute to extreme precipitation.

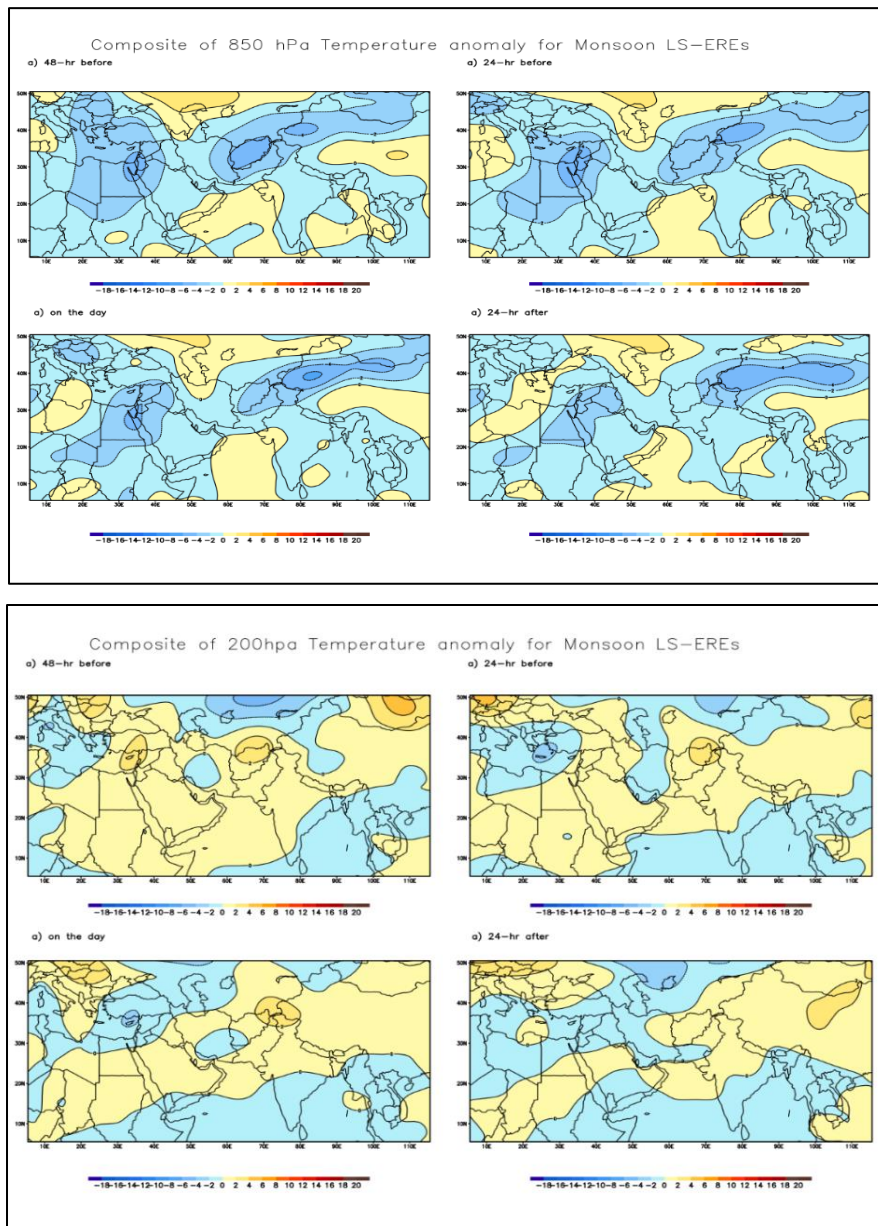
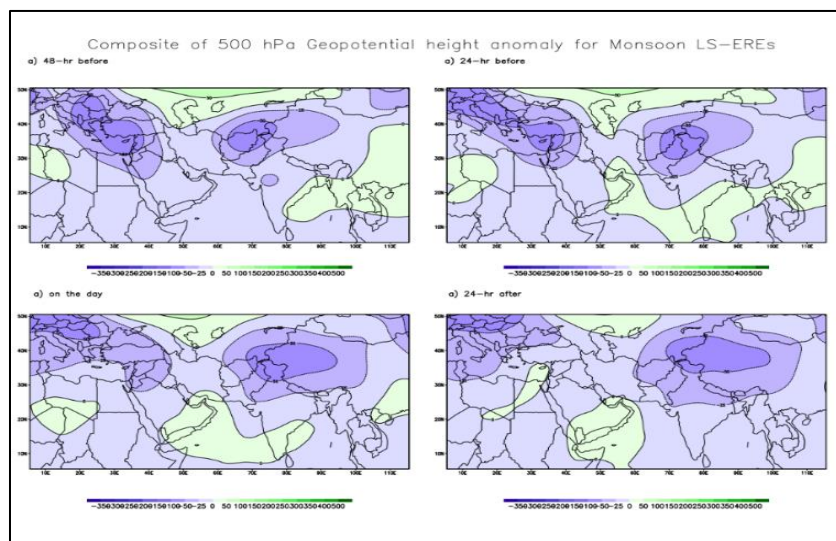
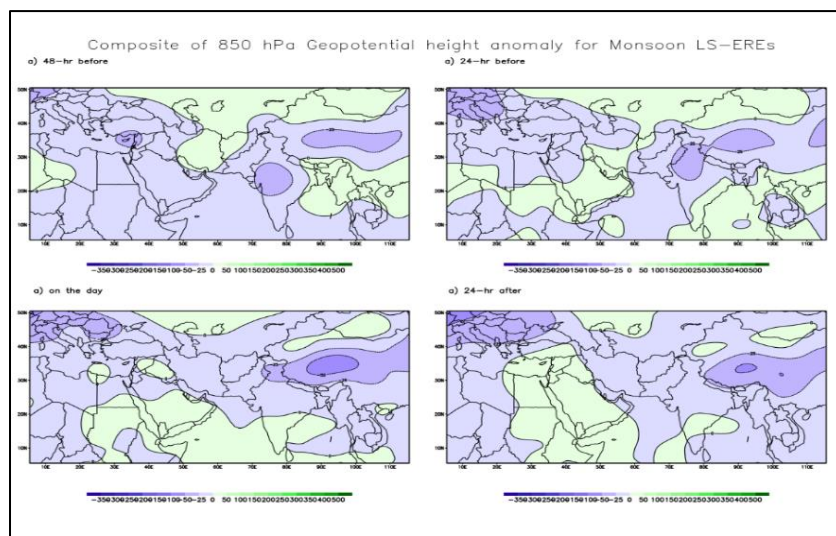


Fig 23. Composites of temperature Anomalies at 850 hpa, and 200hpa prior to, during and after the occurrences of LS-ERE over NWH during monsoon

Composites of gph Anomalies at 850 hpa, 500hPa and 200hpa prior to, during and after the occurrences of monsoon extremes are shown in fig 24. At surface level (850hPa) a negative geopotential height anomaly develops before the event, strengthening on the event day, signifying a deepening low-pressure system and enhanced moisture transport. At mid-level (500hPa), a pronounced negative geopotential height anomaly appears 48 hours before the event, deepening further on the event day, indicating the intensification of a mid-tropospheric trough, which aids in convective activity and precipitation. A strong negative geopotential height anomaly aligns with the mid-level trough, confirming the presence of an upper-level trough and enhanced divergence aloft, further supporting convective uplift. At upper level (200hPa), a strong negative

geopotential height anomaly aligns with the mid-level trough, confirming the presence of an upper-level trough and enhanced divergence aloft, further supporting convective uplift.

The combined effect of lower-level cold anomalies indicating moisture saturation and vigorous convective instability, a mid-level deepening trough that promotes sustained upward motion, and upper-level divergence collectively establishes a favorable baroclinic environment for extreme rainfall. Strengthening of the geopotential height anomaly from the surface to upper levels suggests the development of a well-structured synoptic system, possibly linked to western disturbances or upper-level trough interactions. The anomalies weaken post-event, indicating system dissipation within 24 hours. These findings highlight the role of multi-level interactions between temperature gradients, geopotential height anomalies, and atmospheric instability in driving extreme monsoon rainfall over the Northwest Himalaya.



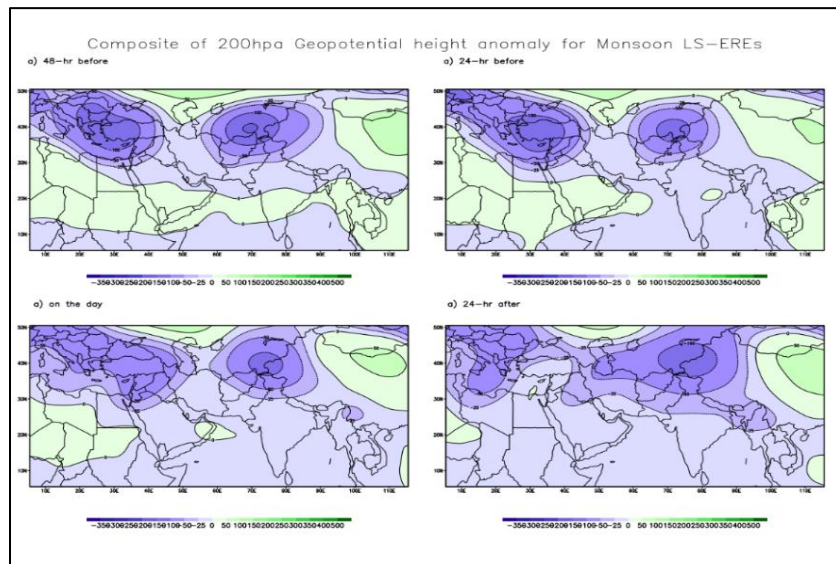


Fig 24 . Composites of geopotential height Anomalies at 850 hpa, 500hPa and 200hpa prior to, during and after the occurrences of LS-ERE over NWH during monsoon

Tropospheric Temperature (1000-250 hPa) and Tropospheric Thickness (1000-250 hPa) anomalies as shown in figure 25 further help elucidate the atmospheric conditions associated with large-scale extreme rainfall events (LS-EREs). 48 hrs before the event, a pronounced negative (cool) anomaly is observed over northwest India, extending towards the Himalayas. This vertically integrated cooling is indicative of large-scale moistening and instability buildup in the troposphere. 24 hrs before the event, cooling intensifies and becomes more spatially coherent over the region of interest. The persistence and intensification of cooling anomalies suggest continued moisture convergence, increased atmospheric saturation, and potential convective instability enhancement. On the day of event, maximum cooling anomalies become most prominent and widespread across northwest Himalayas. These robust tropospheric cooling anomalies typically reflect strong upward motion, intense convective processes, latent heat release, and persistent rainfall. Tropospheric thickness anomalies represent the integrated temperature and moisture state of the entire troposphere, directly reflecting atmospheric stability conditions. Significant negative thickness anomalies (reduced tropospheric thickness) are notable over the northwest Himalayas and adjacent areas 48 hrs before the event, indicating cooler and moister atmospheric columns. Such conditions typically set the stage for vigorous convection. On the event day, the anomalies are deepest and precisely centered over the northwest Himalayas, reinforcing strong vertical motions, deep convection, significant moisture content, and the likelihood of intense rainfall. The co-location with temperature anomalies further emphasizes intense latent heat release during heavy precipitation events.

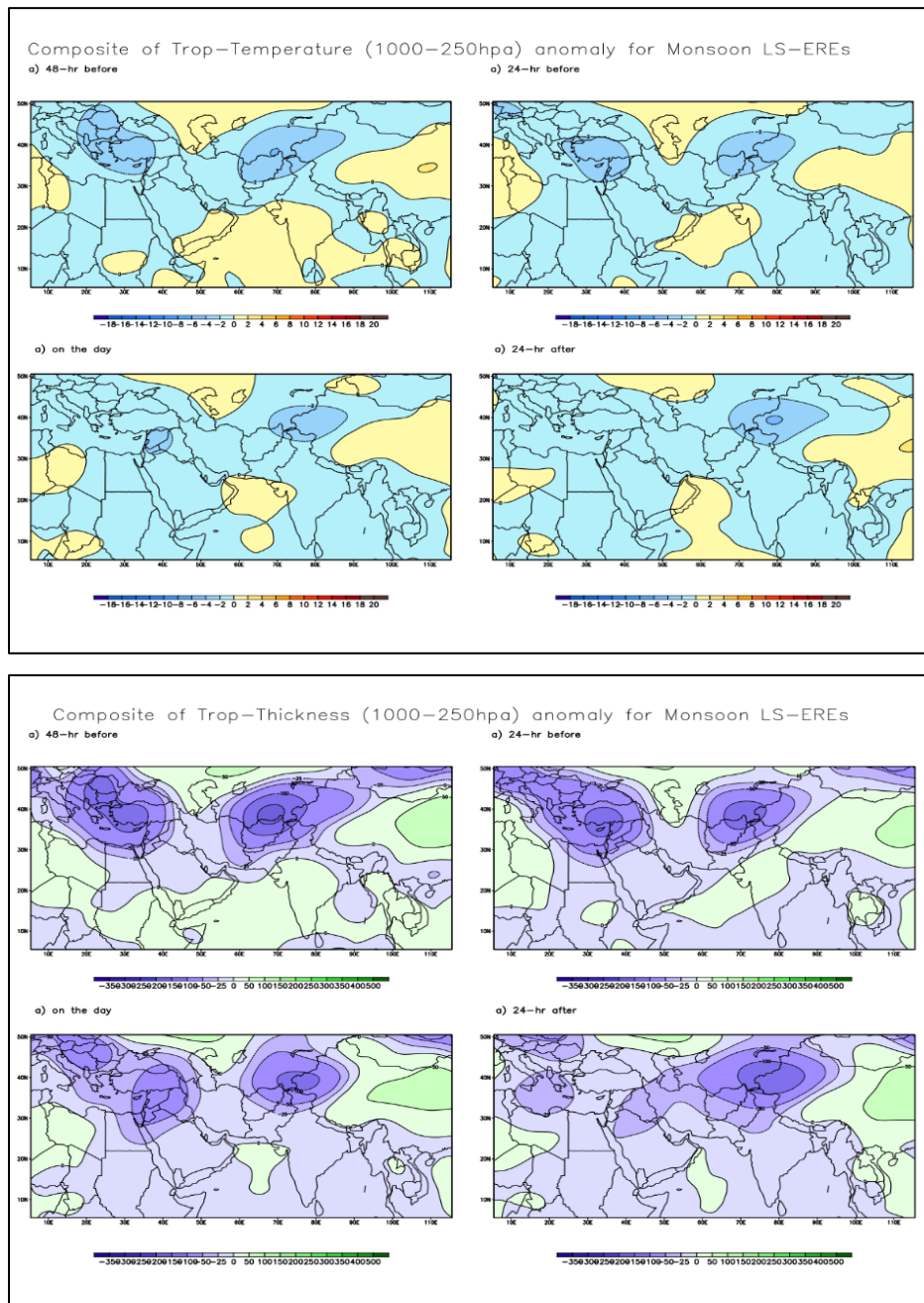


Fig 25. Composites of tropospheric temperature and thickness anomalies prior to, during and after the occurrences of LS-ERE over NWH during monsoon

The consistent pattern of negative anomalies in both tropospheric temperature and thickness clearly underscores that a vertically deep and highly unstable atmospheric column characterized these extreme rainfall events. Intense cooling and thinning suggest vigorous moisture convergence, uplift, deep convection, and latent heat release occurring consistently from lower to upper tropospheric levels. Such conditions are typically associated with strong synoptic-scale forcing (upper-level troughs and low-level

cyclonic circulations), moisture-rich southwesterly monsoon flows, and significant orographic uplift along the Himalayan ranges.

Composite charts for 500 hPa and 200 hPa wind anomalies and relative vorticity are prepared as shown in fig 26. 500hPa charts shows, a notable cyclonic vorticity anomaly (positive vorticity, shown in orange) over the northwestern Indian region, indicating an initial cyclonic circulation and potential mid-level disturbance conducive to rainfall generation. Prominent anticyclonic anomalies (negative vorticity, purple) to the west suggest a blocking pattern facilitating the eastward progression or intensification of cyclonic anomalies towards the northwest Himalayas. The next day, cyclonic vorticity intensifies distinctly over the northwest Himalayas and adjoining plains. Persistent anticyclonic anomalies to the west act as an amplifying agent by reinforcing the mid-level cyclonic anomaly, maintaining its intensity and slow progression. On day of the event, well organized cyclonic anomalies are observed over NW Himalaya strongly indicative of mid-level convergence, enhanced lifting mechanisms, and robust convective activity directly leading to intense rainfall. At 200 hPa level, 48 hr before the event, a strong anticyclonic (negative) vorticity anomaly is seen northward over Central Asia, suggesting a pronounced upper-level ridge/blocking feature. Such anticyclonic conditions northward typically enhance jet stream dynamics over the Himalayas, supporting upper-level divergence downstream. Broad-scale negative anomalies (anticyclonic) are noted over adjacent regions, indicating large-scale upper-level steering and divergence mechanisms preparing the conditions for intensified rainfall. The next day, upper-level anticyclonic anomalies intensify northward, establishing a strong gradient and divergence over the northwest Himalayas. On the day of event, robust and extensive anticyclonic anomalies dominate north of the Himalayas and over Central Asia, maintaining persistent upper-level divergence downstream. Enhanced divergence at 200 hPa directly above the region of extreme rainfall provides essential dynamical support for deep convection, lifting, and intense precipitation.

Mid-level cyclonic circulation (500 hPa) creates consistent convergence and intense vertical motions, and moisture pooling. Upper-Level anticyclonic divergence (200 hPa) crucial for dynamically sustaining the lower-to-mid-level convective processes. The synergy between persistent mid-level cyclonic circulation and strong upper-level divergence structures a highly favorable dynamic environment for intense vertical motions, sustained convection, and heavy precipitation.

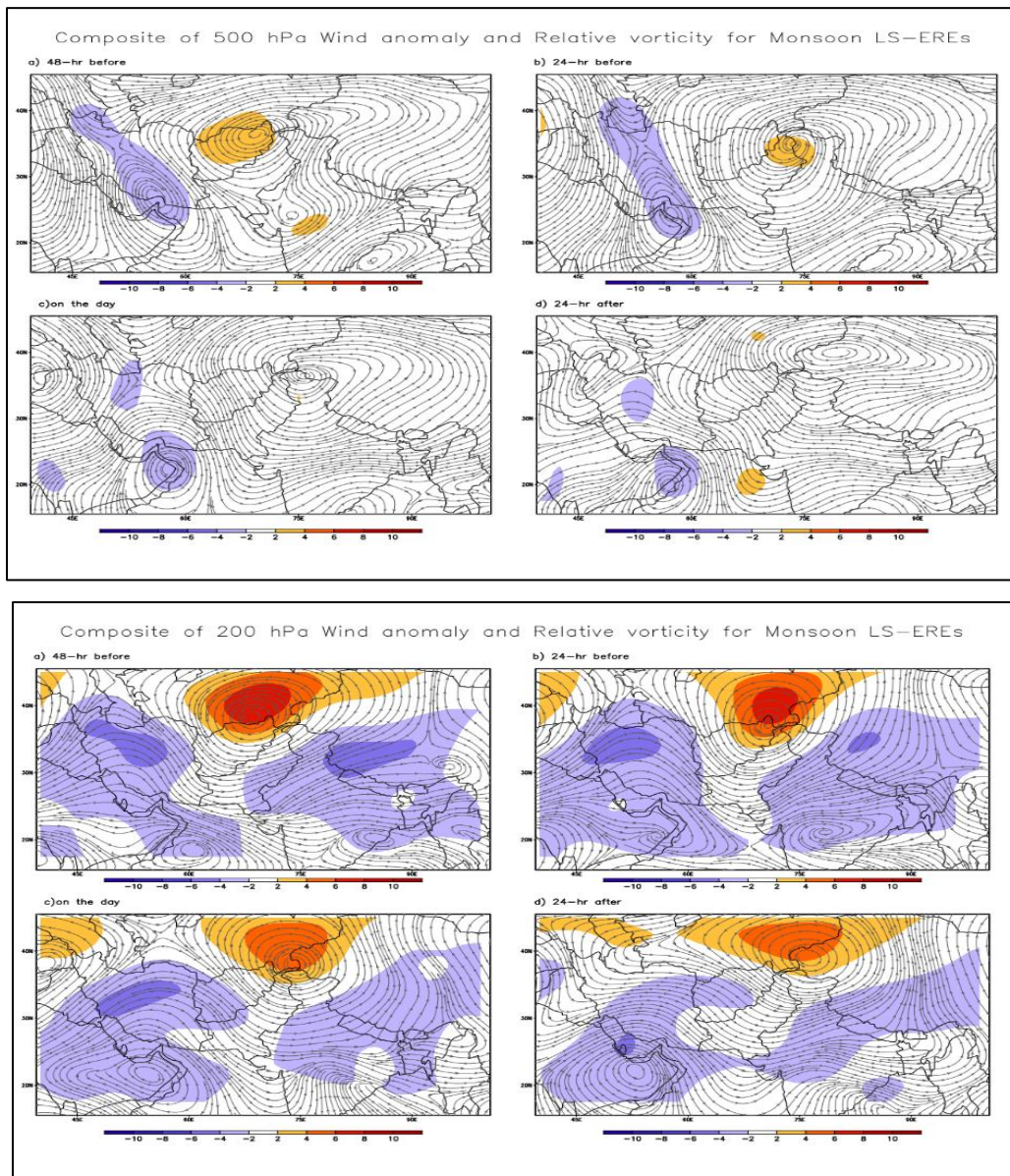


Fig 26. Composites of wind anomalies and relative vorticity at 500hPa and 200hPa prior to, during and after the occurrences of LS-ERE over NWH during monsoon

Fig 27 shows normal GWR during monsoon as well GWRs composites of monsoon extremes at 850hPa, 600hPa, 400hPa and 200hPa. In normal monsoon picture, lower-level WL anomalies combined with strong upper-level WH anomalies are clearly visible. Ideal conditions for deep convection and typical monsoon rainfall patterns across India, with a well-organized monsoon trough at lower and mid-levels, and the TEJ and associated divergence aloft.

During extreme condition, at lower tropospheric levels (850 hPa and 600 hPa), extensive Warm-Low (WL) regimes dominate across the Indian subcontinent and adjacent oceanic regions. This strongly indicates warm, moist conditions enhancing convective instability typical of the Indian monsoon. Warm-Low anomalies are highly pronounced and extensive compared to winter, reflecting the strong heating and

moisture availability typical of monsoonal conditions. At mid to upper levels (400 hPa and 200 hPa), strong vertical continuity of Warm-Low anomalies clearly continues from lower to mid-tropospheric levels. This intensification signifies deep atmospheric instability and strong moisture-laden ascent throughout the tropospheric column. Considerable presence of Warm-High and Cool-High regimes are notable across subtropical and mid-latitude regions, implying strong anticyclonic features which are characteristic of the upper-tropospheric monsoon anticyclone. Such features indicate a strengthened and northward-extended tropical easterly jet (TEJ), crucial for providing favorable divergence aloft necessary for heavy rainfall events.

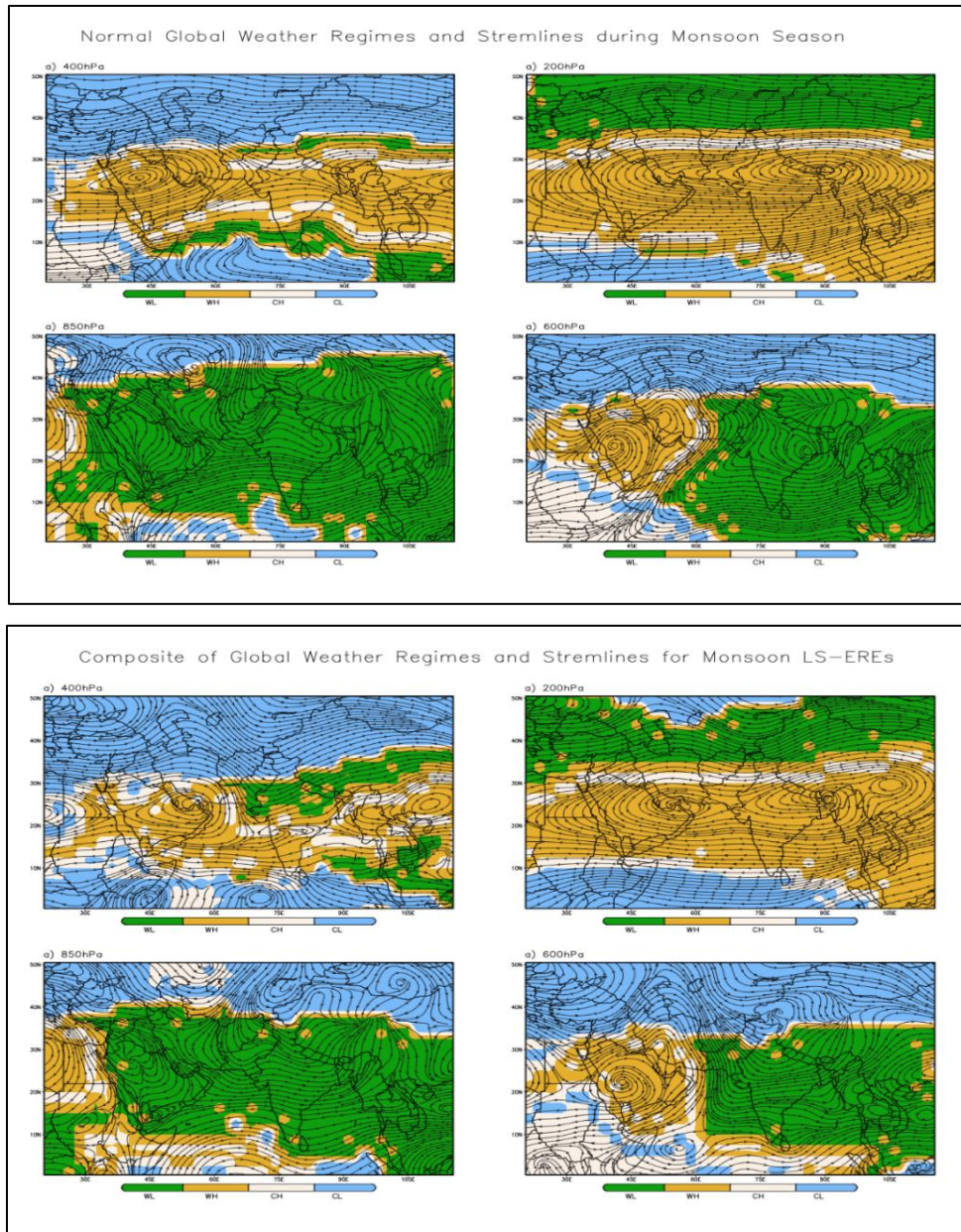


Fig 27 Normal Global weather regimes at 850 hPa, 600hPa, 400hPa and 200hpa during monsoon and composites for the occurrences of LS-EREs over NWH during monsoon

Interaction of warm-high and cool-high at the NW Himalaya can be easily noticed in mid tropospheric level. Clearly visible monsoon trough and cyclonic vortices at lower levels (850 hPa), ensuring sustained moisture convergence and deep convection over Northwest Himalaya. Upper-level easterlies (200 hPa) demonstrate the strength and northward displacement of the TEJ, strongly correlated with monsoon rainfall intensity. Monsoon-season large-scale extreme rainfall events over NW Himalaya are fundamentally governed by lower-level moist convection, monsoon trough positions, and pronounced upper-level divergence facilitated by the TEJ.

The marked contrasts in regimes (low-level WL vs upper-level WH-CH interface) provide robust thermodynamic and dynamic conditions conducive to intense rainfall. During monsoonal ERE days, wide spread cold anomalies and a negative geopotential height anomaly at lower level enhance moisture convergence and low-pressure deepening. Upper-level cooling, negative geopotential height anomalies, and upper-level divergence (due to jet stream interaction) drive extreme vertical motion and heavy precipitation. The unusual and abrupt warming of the upper troposphere in the Tibet and Turkey sectors promotes the development of deep troughs and reinforced ridges in subtropical westerlies. The abrupt intensification of the monsoon circulation connected to this warming causes catastrophic spatio-temporal rain events across NWH. Monsoon LS-EREs over NWH are driven by a multi-layer interaction of cold anomalies, deepening low pressure, mid-level troughs, and upper-level divergence. Baroclinic instability, jet stream interactions, and cyclonic vorticity are key factors that intensify these extreme rainfall events. The system evolves in a vertically stacked manner, with peak intensity on the event day and dissipation within 24 hours.

4.8.3 KEY DIFFERENCES BETWEEN WINTER AND MONSOON LS-ERES

- Winter extremes are distinctly characterized by deep vertically stacked cool-low anomalies, intensified cyclonic circulation due to western disturbances, and robust upper-tropospheric divergence driven by amplified jet streams and troughs. Crucially, they occur without prominent low-level warm anomalies typically associated with monsoon-driven extremes. They are primarily driven by mid-latitude dynamics (baroclinic processes, western disturbances, jet stream dynamics), rather than tropical convective mechanisms dominant during the monsoon. While Monsoon EREs shows strong negative temperature (cooling) and deep negative geopotential height anomaly at lower level, indicative of active convection, low-level moistening, and latent heat release. At upper level, prominent trough and divergence is seen during monsoon and strong jet and Rossby wave pattern observed during winter EREs.
- Vertical coupling is often shallower and primarily in mid/upper levels during winter EREs while it is throughout troposphere during monsoon extremes.

- Atmospheric instability during winter extremes is mainly dynamic, driven by baroclinic instability and cold air advection, while during monsoon it is thermodynamic and driven by moisture convergence, convection, and monsoon troughs.
- Because of above mentioned peculiarities, the predictability of winter extremes is better due to well-developed WDs while that of monsoon are moderate that depends on monsoon circulation.

5. IMPORTANT RESULTS:

1. The annual, monsoonal and other seasonal rainfall series of NWH are homogenous and random. No significant long-term trend is noticed in any of the series during 1951-2021. In recent 20 years (2001-2021), OND rainfall of NWH has decreased significantly by 25% compare to preceding 51 years record.
2. No significant long-term trend is observed in annual and monsoonal rainfall series of Uttarakhand, however OND rainfall shows significant decreasing long-term trend during 1951-2021. In recent 20 years, it has decreased significantly by 35% compare to preceding 51 years record.
3. Significant decreasing long-term trend is observed in annual rainfall of Himachal Pradesh during 1951-2021, however other seasonal rainfall series are homogeneous and random. In recent 20 years, annual rainfall of HP decreased by ~13%, monsoon by ~8.5%, OND by ~33%, JF by 17% and MAM by ~17% respectively
4. Significant increasing long-term trend is observed in JF rainfall of Jammu and Kashmir during 1951-2021, however annual and other seasonal rainfall series are homogeneous and random. In recent 20 years, monsoon rainfall of J&K increased by ~18% compare to preceding period.
5. Normally rainfall amount of large-scale ERE-RA of 1- to 10-day duration increases from 58mm to 203.36mm, over NWH, 71.5mm to 148.1mm over UK, 57mm to 206.8mm over HP and 58.5mm to 175.2mm over J&K state.
6. During 1951-2021, over J&K, AE of 1- to 7-days ERE-RA and RW of 1- to 2-day ERE-RW of shows significant increasing trend. Over HP, RA of 3- to 10-days ERE-RA and RW of 4-10 day ERE-RW shows significant decrease.
7. Over UK state, rainfall amount of large-scale EREs of different durations increased by 10-23% and rainwater by 14-34% in recent 20 years. Over J&K state, rainfall amount of 1-day large-scale ERE-RA increased by 16% and rainwater of ERE-RW by 23%, while areal extent of different durations by 19-23% in recent 20 years. Over HP, rainfall amount of large-scale ERE-RA of different durations decreased by -10-20% and rainwater by -14 to -19% in recent 20 years. Over NWH as a whole, no significant change is seen in RA of ERE-RA, but the areal extent of 1-3 day duration EREs significantly increased by 28-43% and rainwater of 1-day ERE-RW by 16% in recent 20 years.

8. Winter extremes are distinctly characterized by deep vertically stacked cool-low anomalies, intensified cyclonic circulation due to western disturbances, and robust upper-tropospheric divergence driven by amplified jet streams and troughs.
9. Monsoon EREs associated with active convection, low-level moistening, and latent heat release driven by moisture convergence, convection, and monsoon troughs.

6. CONCLUSIONS

Increasing rainfall amounts, rainwater, and areal extent, highlighting intensified extreme rainfall events over J&K and UK states and declining rainfall amounts and rainwater, signalling a reduction in extreme rainfall activity in HP. No overall change in rainfall totals for NWH, but a significant increase in areal extent of short-duration extreme rainfall events that reflect as increase in rainwater in recent years. The year-wise most severe large-scale EREs mostly occurred during monsoon season, however, surprisingly in some years, the severity and areal extent of non-monsoonal extremes surpassed the monsoon extremes especially over HP and J&K. Short-duration EREs in high-altitude areas are intensified while prolonged rainfall in lower regions are reduced. High intensity EREs (>8 DMR) are less frequent and mostly occur in northern J&K and high-altitude southern regions of HP and UK. Winter LS-EREs are driven by the alignment of low-level low pressure, a mid-level trough, and upper-level divergence forming a vertically stacked system, indicating a well-structured western disturbance. Monsoon LS-EREs have an alignment of warm moist low convective zone at the lower level and warm-moist upper-level divergence indicate convective instability, moisture transport and transient monsoon circulation.

7. IMPLICATIONS TO REGIONAL HYDROLOGY AND DISASTER RISK MANAGEMENT

1. Intense rainfall associated with monsoonal low-pressure systems, moisture convergence, and upper-level divergence can lead to flash floods, riverine floods, and landslides in mountainous regions. Understanding temperature and geopotential height anomalies helps in early identification of extreme rainfall events, aiding flood forecasting in river basins like the Indus, Ganges, and Yamuna.
2. Extreme precipitation in winter (snowfall or rainfall) due to Western Disturbances (WDs) and cold air intrusions can result in snow accumulation and subsequent snowmelt-induced flooding during spring. Analyzing upper-level vorticity and jet stream interactions can improve snowmelt flood prediction models.
3. Monsoon extreme events contribute significantly to groundwater recharge in the Himalayan foothills and alluvial plains. While, winter extreme events influence seasonal water availability through snowfall and glacier mass balance, which impacts summer runoff and water supply for agriculture and drinking purposes.

4. Forecasting of Extreme rain events can be enhanced by using temperature/ geopotential height anomalies, while GWR analysis will help in identification of location of occurrences of LS-EREs and their intensification. That help regional disaster management authorities issue timely warnings to vulnerable communities.
5. Monsoon LS-EREs often trigger landslides due to prolonged heavy rainfall saturating the soil while winter LS-EREs contribute to glacier surges and avalanches. The study helps the authorities to identify regions at higher risk and implement mitigation measures such as slope stabilization, improved drainage systems, and flood barriers.
6. Meteorological analysis of the evolution and genesis of severe EREs will be helpful in improving the physical processes in numerical weather prediction models and to develop early warning systems.
7. Analysis of various types of extremes over an extended period helps scientists to understand changing precipitation patterns due to climate change over NW Himalaya. The analysis provides insights into how climate change is altering the frequency and intensity of extreme events over the NWH. Warmer temperatures could shift precipitation patterns, increasing rain-on-snow events, which accelerate glacier melt and extreme runoff.
8. Understanding seasonal variability in precipitation extremes can help policymakers and water managers optimize reservoir operations, irrigation planning, and hydropower generation.
9. High-resolution climate data from these studies can guide infrastructure development (e.g., climate-resilient roads, flood-resistant housing, and improved drainage systems in flood-prone areas). Policymakers can design early warning dissemination systems for communities in high-risk zones.
10. Reservoir inflow forecasting based on extreme event analysis allows better water storage and discharge management in hydropower projects in the Himalayas. Early warning systems for dam operators can prevent reservoir overflow-induced flooding during extreme rainfall events.

REFERENCES:

- Chevuturi A, Dimari AP (2016) Investigation of Uttarakhand (India) disaster-2013 using weather research and forecasting model. *Nat Hazards* 82(3):1703–1726.
- Cho C, Li R, Wang S, Yoon JH, Gillies, RR (2015) Anthropogenic footprint of climate change in the June 2013 northern India flood. *Plants, Soils, and Climate Faculty Publications*. Paper 735, 26pp.
- Dube A, Ashrit R, Ashish A, Sharma K, Iyengar GR, Rajagopal EN, Basu S (2014) Forecasting the heavy rainfall during Himalayan flooding-June 2013. *Weather Clim Extremes* 4:22–34
- Houze RA, McMurdie LA, Rasmuseen KL, Kumar A, Chaplin MM (2017) Multiscale aspects of the storm producing the June 2013 flooding in Uttarakhand, India. *Mon Wea Rev* 145(11):4447– 4466. <https://doi.org/10.1175/MWR-D-17-0004.1>
- IPCC (2007) *Climate change 2007: the physical science basis. Contribution of working group I to the fourth assessment report of the intergovernmental panel on climate change*. Cambridge University Press, Cambridge, pp 504–511
- IPCC (2021) ‘Climate Change 2021. The physical science basis’, Working Group I Contribution to the Sixth Assessment Report of the Intergovernmental Panel on Climate Change. Cambridge, UK: Cambridge University Press, In Press.
- Joseph S, Sahai AK, Sharmila S, Abhilash S, Borah N, Chattopadhyay R, Pillai PA, Rajeevan M, Kumar A (2015) North Indian heavy rainfall event during June 2013: diagnostics and extended range prediction. *Clim Dyn* 44:2049–2065.
- Kotal SD, Roy SS, Bhowmik SKR (2014) Catastrophic heavy rainfall episode over Uttarakhand during 16–18 June 2013—observational aspects. *Curr Sci* 107(2):234–245
- Krishnamurti TN, Kumar V, Simon A, Thomas A, Bhardwaj A, Das S, Sen Roy S, Roy Bhowmik RK (2017) March of buoyancy elements during extreme rainfall over India. *Clim Dyn* 48:1931–1951
- Priya P, Krishnan R, Mujumdar M, Houze RA Jr (2017) Changing monsoon and midlatitude circulation interactions over the Western Himalayas and possible links to occurrences of extreme precipitation. *Clim Dyn* 49:2351–2364.
- Ranade, A. & Singh, N. (2014) Large-scale and spatio-temporal extreme rain events over India: a hydrometeorological study, *Theoretical and Applied Climatology*, 115, 375–390.
- Ranade A, Singh N (2019) Equatorially/Globally conditioned meteorological analysis of heaviest rains over India during 23–28 July 2005. *Meteorol Atmos Phys* 131(4):919–944. <https://doi.org/10.1007/s00703-018-0613-6>

- Ranade, A. & Singh, N. (2021) Evaluation of 3D structural changes in general atmospheric and monsoon circulations during Kedarnath disaster (India), 16–17 June 2013, *Meteorology and Atmospheric Physics*, 133, 857–878.
- Ranalkar MR, Chaudlhari HS, Hazra A, Sawaisarje GK, Pokhrel S (2016) Dynamical features of incessant heavy rainfall event of June 2013 over Uttarakhand, India. *Nat Hazards* 80:1579–1601.
- Saha S et al (2010) The NCEP climate forecast system reanalysis. *Bull Am Meteorol Soc* 91(8):1015–1057. <https://doi.org/10.1175/2010BAMS3001.1>
- Saha S et al (2014) The NCEP climate forecast system version 2. *J Clim* 27:2185–2208. <https://doi.org/10.1175/JCLI-D-12-00823.1>
- Shekhar MS, Pattanayak S, Mohanty UC, Paul S, Sravana Kumar SM (2015) A study on the heavy rainfall event around Kedarnath area (Uttarakhand) on 16 June 2013. *J Earth Syst Sci* 124(7):1531–1544.
- Singh D, Horton DE, Tsiang T, Haugen M, Ashfaq M, Mei R, Rastogi D, Johnson NC, Charland A, Rajaratnam B, Diffenbaugh NS (2014) Severe precipitation in Northern India in June 2013: causes, historical context, and changes in probability. *Bull Am Meteorol Soc* 95(9):558–561.
- Srinivasan J (2013) Predicting and managing extreme rainfall. *Curr Sci* 105:7–8
- Senior CA, Jones RG, Lowe JA, Durman CF, Hudson D (2002) Predictions of extreme precipitation and sea-level rise under climate change. *Phil Trans R Soc Lond A* 360:1301–1311
- Vellore RK, Kaplan ML, Krishnan R, Lewis JM, Sabade S, Deshpande N, Singh BB, Madhura RK, Rama Rao MVS (2016) Monsoonextratropical circulation interactions in Himalayan extreme rainfall. *Clim Dyn* 46:3517–3546

~~~~~